The structure and rate of late Miocene expansion of C_4 plants: Evidence from lateral variation in stable isotopes in paleosols of the Siwalik Group, northern Pakistan

Anna K. Behrensmeyer*
Department of Paleobiology, MRC 121, National Museum of Natural History, Smithsonian Institution, P.O. Box 37012, Washington, DC 20013-7012, USA

Jay Quade
Dept. of Geosciences and the Desert Laboratory, University of Arizona, Tucson, Arizona 85721, USA

Thure E. Cerling
Dept. of Geology and Geophysics, University of Utah, Salt Lake City, Utah 84112, USA

John Kappelman
The University of Texas at Austin, Department of Anthropology, University Station C3200, Austin, Texas 78712, USA

Imran A. Khan
Deputy Director General, Geological Survey of Pakistan, Jauhar Town, Phase–II, Lahore, Pakistan

Peter Copeland
Department of Geosciences, University of Houston, Houston, Texas 77204, USA

Lois Roe
907 Eton Way, Neptune, New Jersey 07753, USA

Jason Hicks
Denver Museum of Nature and Science, 2001 Colorado Blvd., Denver, Colorado 80205, USA

Phoebe Stubblefield
Forensic Science Department, Babcock Hall, Room 208, University of North Dakota, Grand Forks, North Dakota 58202, USA

Brian J. Willis
Shallow Marine Stratigraphy, Chevron Energy Technology Company, 1500 Louisiana St., Houston, Texas 77002, USA

Claudio Latorre
CASEB-Departamento de Ecología, Pontifica Universidad Católica de Chile, Santiago 114-D and Institute of Ecology & Biodiversity, Las Palmera 3425, Santiago, Chile

ABSTRACT

This study uses stable isotope variation within individual Mio-Pliocene paleosols to investigate subkilometer-scale phytogeography of late Miocene vegetation change in southeast Asia between ca. 8.1 and 5 Ma, a time interval that coincides with dramatic global vegetation change. We examine trends through time in the distribution of low-latitude grasses (C_4 plants) and forest (C_3 plants) on Indo-Gangetic floodplains using carbon ($\delta^{13}C$) and oxygen isotopic ($\delta^{18}O$) values in buried soil carbonates in Siwalik Series sediments exposed in the Rohtas Anticline, north-central Pakistan. Revised, high-resolution magnetostratigraphy and a new $^{40}Ar/^{39}Ar$ date provide improved age control for the 2020 m Rohtas section. Carbon isotope results capture lateral variability of C_3 versus C_4 plants at five stratigraphic levels, R11 (8.0 Ma), R15 (6.74–6.78 Ma), R23 (5.78 Ma), R29 (4.8–4.9 Ma), and upper boundary tuff (UBT; 2.4 Ma), using detailed sampling of paleosols traceable laterally over hundreds of meters. Paleosols and the contained isotopic results can be assigned to three different depositional contexts within the fluvial sediments: channel fill, crevasse-splay, and floodplain environments. $\delta^{13}C$ results show that near the beginning (8.0 Ma) and after (4.0 Ma) the period of major ecological change, vegetation was homogeneously C_3 or C_4, respectively, regardless of paleo-landscape position. In the intervening period, there is a wide range of values overall, with C_4 grasses first invading the drier portions of the system (floodplain surfaces) and C_3 plants persisting in moister settings, such as topographically lower channel swales. Although abrupt on a geologic timescale, changes in abundance of C_4 plants are modest (~2% per 100,000 yr) compared to rates of vegetation turnover in response to

*E-mail: behrensa@si.edu.

GSA Bulletin; November/December 2007; v. 119; no. 11/12; p. 1486–1505; doi: 10.1130/B26064.1; 12 figures; 1 tables; Data Repository item 2007282.

glacial and interglacial climate changes in the Quaternary. Earlier research documented a sharply defined C_3 to C_4 transition in Pakistan between 8.1 and 5.0 Ma, based on vertical sampling, but this higher-resolution study reveals a more gradual transition between 8.0 and 4.5 Ma in which C_3 and C_4 plants occupied different subenvironments of the Siwalik alluvial plain.

$\delta^{18}O$ values as well as $\delta^{13}C$ values of soil carbonate increase up section at Rohtas, similar to isotope trends in other paleosol records from the region. Spatially, however, there is no correlation between $\delta^{13}C$ and $\delta^{18}O$ values at most stratigraphic levels. This implies that the changes in soil hydrology brought about by the shift from forest to grassland (i.e., an increase in average soil evaporation) did not produce the shift through time in $\delta^{18}O$ values. We interpret the trend toward heavier soil carbonate $\delta^{18}O$ values as a response to changes in external climatic factors such as a net decrease in rainfall over the past 9 Ma.

Keywords: carbon isotopes, oxygen isotopes, paleosol, Miocene, Pakistan.

INTRODUCTION

Stable isotopes preserved in ancient soils are being used to track vegetation and climate changes through time within many different Cenozoic rock sequences (Quade and Cerling, 1995; Cerling et al., 1997; Latorre et al., 1997; Kleinert and Strecker, 2001; Fox and Koch, 2004; Levin et al., 2004; Wynn, 2004). These stable isotope records typically are based on vertical sampling through long stratigraphic sequences, and each sample is assumed to represent average $\delta^{13}C$ and $\delta^{18}O$ values for that time interval. Lateral variations in $\delta^{13}C$ and $\delta^{18}O$ at a given point in time have seldom been documented but could provide information on vegetation complexity that contributes to more detailed ecological reconstructions of evolving paleo-landscapes (Sikes 1994; Levin et al., 2004).

A major shift from C_3 to C_4 vegetation between ca. 8.0 and 5.0 Ma was previously documented in the Siwalik Series of northern Pakistan (Quade and Cerling, 1995; Cerling et al., 1997; Quade and Roe, 1999). The goal of this paper is to refine understanding of this isotope shift (hereafter termed the "Siwalik C_3-C_4 transition") by examining phytogeographic patterns of the C_4 grass expansion using stable isotopic evidence from carbonates in alluvial paleosols. We differ from all previous studies of the C_4 grass expansion in Pakistan in the fine scale of our observations, which are at the outcrop level and based on samples from single paleosols that can be traced laterally over hundreds of meters. These paleosols formed on the aggrading floodplains of large rivers and record vegetation patterns on a portion of the vast sub-Himalayan piedmont alluvial plain at a paleolatitude of ~29–31°N (Opdyke et al., 1979; Tauxe and Opdyke, 1982). Macroplant remains and pollen are poorly preserved in the Pakistan Siwalik Group, and pedogenic carbon isotope values are an important proxy for characteristics of Miocene-Pleistocene paleovegetation.

Stable isotopic evidence from paleosol carbonate, groundwater cements, and fossil teeth shows that C_4 vegetation underwent a dramatic expansion in the late Miocene (Stern et al., 1994; Quade and Cerling, 1995; Cerling et al., 1997, 2003; Morgan et al., 1994; Quade and Roe, 1999; Levin et al., 2004; Nelson, 2007). The timing of this expansion appears to be diachronous globally, occurring first at low latitudes and later at higher latitudes (Cerling et al., 1997). By the Plio-Pleistocene, the expansion was complete in many low-latitude areas. Most C_4 plants are grasses, so this expansion marks the emergence of tropical and temperate latitude grasslands at the expense of C_3 vegetation (woody plants as well as C_3 grasses), which in many places was probably woodland and forest (Quade et al., 1995; Hoorn et al., 2000). Palynological study of the Siwalik sequence in Nepal shows little evidence of grass prior to 7.0 Ma (Hoorn et al., 2000). Based on previous research in Pakistan, the Siwalik C_3-C_4 transition began between 7.8–8.1 Ma and was complete (i.e., most $\delta^{13}C$ values >–2‰) by ca. 5 Ma.

We specifically address the following questions in this paper: (1) what is the lateral variability in pedogenic carbon and oxygen values in Siwalik paleosols and how does this change through time; (2) how does isotopic variability within single paleosols relate to topographic and geologic features of the floodplain environments; (3) what do these results indicate with regard to rates and patterns of vegetation change during the overall C_3-C_4 transition in northern Pakistan; and (4) what are the implications of these isotope trends for understanding the dynamics of this fluvial paleo-ecosystem in particular and environmental change in general?

To address these questions we studied Siwalik Group deposits in the Potwar Plateau, which are exposed in a series of shallow anticlines in the Jhelum syntaxis (Fig. 1) at the eastern end of the Salt Range. One of these, the Rohtas anticline, provides continuous exposures with abundant paleosols through the interval of the C_3-C_4 transition in southern Asia, between 8.1 and 5.0 Ma. The Rohtas section contributed to original documentation of the Siwalik C_3-C_4 transition in Pakistan (Quade et al., 1989a), with previous age information based on magnetostratigraphy and radiometric dating of several volcanic ashes that occur in its upper part (Opdyke et al., 1979; 1982; GSA Data Repository item part one[1]). In this paper, we report new magnetostratigraphic results and an $^{40}Ar/^{39}Ar$ date for the Rohtas section that allow more secure correlations to the geomagnetic reversal time scale (GRTS) and provide better calibration of the timing and rate of the Siwalik C_3-C_4 transition and the age of paleosol carbonates used in this and previous studies.

GEOLOGIC SETTING

The Siwalik Group occurs continuously from Afghanistan and western Pakistan to Burma and consists of fluvial sediments deposited in the foreland basin formed by the collision of the Indian subcontinent with Asia over the past 18 Ma. Miocene strata are faulted and folded adjacent to and south of the overthrust belt, resulting in widespread exposures of sedimentary rocks, which are rich in vertebrate fossils. The Siwalik Group in Pakistan consists of five formations (Kamlial, Chinji, Nagri, Dhok Pathan, and Soan), amounting to a total thickness of >4 km in the Potwar-Kohat depression in Pakistan (Tauxe and Opdyke, 1982; Johnson et al., 1985). In the Potwar area, the chronostratigraphy is based on paleomagnetism, supplemented by isotopic dating of rare volcanic ash beds (Johnson et al., 1982a, 1982b, 1985). The formations are characterized by different proportions of sand versus mudstone, reflecting shifts through time in the geographic position of large- to small-scale rivers and their alluvial deposits as well as changes in foreland basin subsidence and sediment input (Burbank and Beck, 1991; Willis, 1993a, 1993b; Khan et al., 1986, 1997; Zaleha, 1997). Studies of the fluvial sedimentology of the Miocene through Pleistocene deposits document the changing influence of mountain (Himalaya)-sourced ("blue-gray") versus lowland-sourced ("buff") rivers (Raynolds, 1981; Behrensmeyer and Tauxe 1982; Burbank and Beck, 1991; Barry et al., 2002). These studies provide specific information on flow directions and velocities, channel size and geometry, and floodplain aggradation. Paleochannel belts in the Jhelum area were on

[1]GSA Data Repository item 2007282, data repository part 1: Paleomagnetic chronostratigraphy and radiometric dating results (text, Tables DR1–DR3, and Figures DR1–DR5); data repository part 2: Stable isotope results (Tables DR4 and DR5); and data repository part δ: $\delta^{13}C$ vs. $\delta^{18}O$ Correlations (Figures DR6–DR14 and Tables DR6–DR8), is available on the Web at http://www.geosociety.org/pubs/ft2007.htm. Requests may also be sent to editing@geosociety.org.

the order of 1.5–2.0 km wide, with individual channels 200–400 m wide and 4–22 m deep (Khan et al., 1997). These channel belts were major east to southeast flowing tributaries to the axial system of the foreland basin, which is not exposed in the Potwar region and presumably was farther south (Khan et al., 1997; Zaleha, 1997). The fluvial systems were characterized by frequent avulsion and channels were dominantly braided or anastamosing rather than meandering (Burbank and Beck 1991; Willis 1993a, 1993b; Willis and Behrensmeyer, 1994; Behrensmeyer et al., 1995). Floodplains were built by overlapping, soil-capped, crevasse-splay deposits rather than classic meander-belt overbank sedimentation (Behrensmeyer et al., 1995).

The total measured thickness of the Siwalik Group exposed in our study area at Rohtas is ~3 km (Opdyke et al., 1979); these deposits span the time interval from ca. 9.4 to 0.5 Ma. Fluvial conglomerates, sandstones, and mudstones are almost continuously exposed along two major dry washes ("kas"), Dhabwala Kas and Basawa Kas (Figs. 1 and 2). Our sampling there was confined largely to five intervals: R11 (8.0 Ma), just below the beginning of the carbon isotopic shift; R15 (6.7–6.8 Ma); R23 (5.8 Ma); R29 (4.8 Ma), within the carbon isotope "transition" interval; and UBT (upper boundary tuff); (2.4 Ma) above the transition (Figs. 2 and 3).

The Rohtas sequence has sandstones representing the blue-gray and the buff fluvial systems that are recognized in other areas of the Potwar (Raynolds, 1981; Behrensmeyer and Tauxe, 1982). At Rohtas, blue-gray sands dominate the lower 250 m and buff sands dominate above 600 m, with an intervening zone of alternating sand compositions (Fig. 2). The blue-gray sands are somewhat thinner than the buff sands, even in the zone of overlap, indicating relatively weak (perhaps marginal) influence of the blue-gray fluvial system in this area.

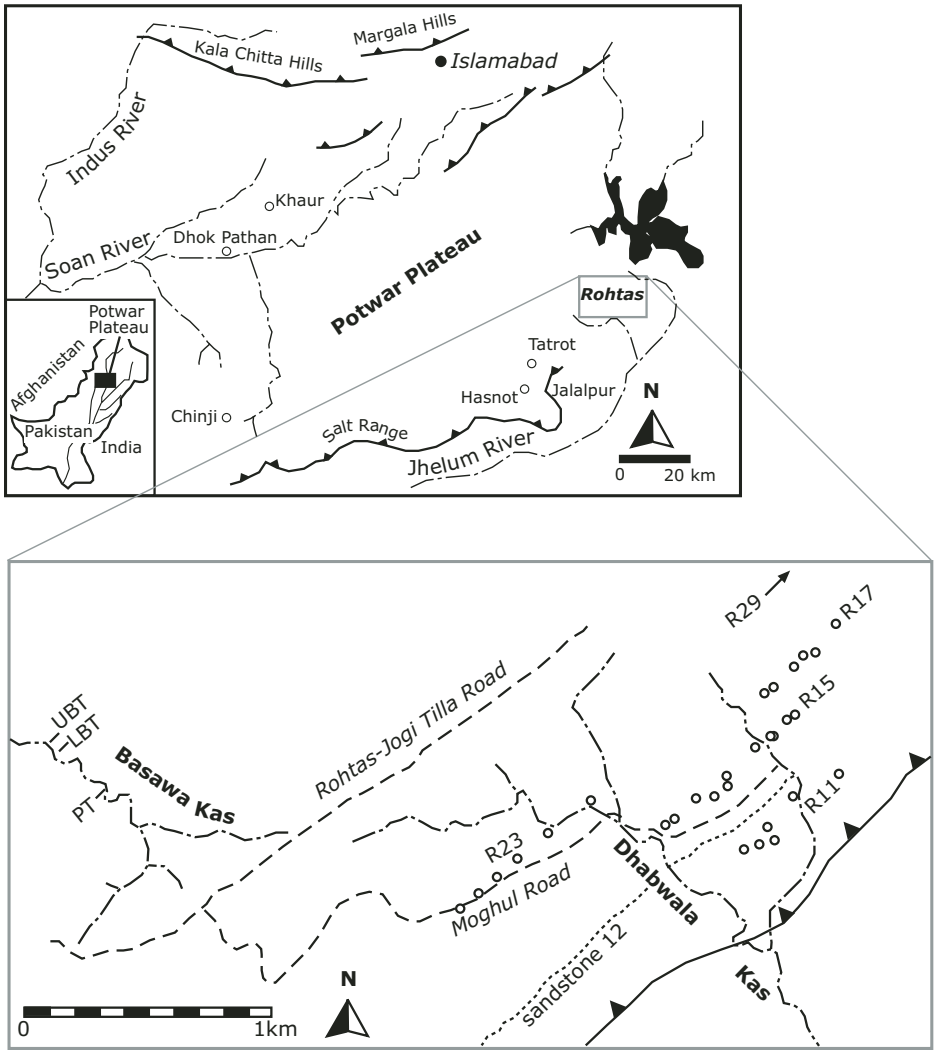

Figure 1. Geography of the Rohtas study area, with upper map showing its location in Pakistan in the southeastern Potwar Plateau (rectangle). Rohtas map (lower) shows the major modern drainages (Dhabwala Kas, Basawa Kas) and positions of panels (R11-R29); open dots show sections and sampling sites along strike. LBT—Lower Boundary Tuff; PT—Pothi Tuff; UBT—Upper Boundary Tuff (Opdyke et al., 1979). Note: Panel R17 yielded few usable isotopic results and was excluded from analysis for this paper.

METHODS

Field Documentation and Sample Collection

Five different levels within the 2020-m-thick Rohtas section (Figs. 2 and 3) were sampled using a coordinated approach in which team members simultaneously documented the field characteristics of the lithostratigraphy and paleosols and collected samples for isotopic and paleomagnetic analysis. Additional samples of carbonate from paleosols stratigraphically below, above, and between these five levels (collected by J. Quade, T.E. Cerling, and A.K. Behrensmeyer) were used to document the overall isotopic trends (Quade and Cerling, 1995).

Lithostratigraphic panels at each of the five target levels in the Rohtas sequence provide the framework for the lateral paleosol study (Fig. 4). These panels were constructed from measured sections 100–200 m apart and 25–40 m thick, linked by lateral tracing of continuous marker beds plus matching of distinctive strata across short covered intervals. Rock type, color, bedding features, and matrix reaction to 10% HCl were recorded consistently through each section at a decimeter scale. The pedogenic features of specific, laterally traceable paleosols were recorded every 20 cm vertically in excavated trenches and include sediment type and grain size, matrix reaction to 10% HCl, color, abundance of carbonate and iron-manganese nodules, clay cutans, slickensides, and root and burrow traces. Although most panels include major sandstone bodies that can be traced laterally for hundreds of meters, paleosols are more consistent in lithologic features and thickness from section to section; hence the upper surfaces of one or more paleosols per section were used as horizontal datums.

Within each target paleosol (Table 1), at least one sample of pedogenic carbonate and/or matrix was taken at each section, resulting in up to 13 lateral sites documenting isotopic variation within the paleosol. In some cases, four or more samples were collected vertically through 1–3 m in the same paleosol to document any vertical trends in isotope values. We sampled

two paleosols within a few square meters on subvertical excavated outcrop surfaces ("grid samples") to test for fine-scale variation in isotopic values and pedogenic features.

Stable Isotopes

Soil carbonate nodules were roasted under vacuum at 400–430 °C prior to conversion to CO_2 with 100% phosphoric acid. Percent carbonate in samples (Table 1; Data Repository item part 2; see footnote 1) was calculated from manometric yields of CO_2. Isotopic analyses were performed on a Finnigan Delta-S gas-source mass spectrometer at the University of Arizona. Results are presented in the usual δ notation as the per mil (‰) deviation of the sample CO_2 from the Peedee belemnite (PDB) standard, where R = $^{13}C/^{12}C$ or $^{18}O/^{16}O$, and δ = $(R_{sample}/R_{standard}-1) \times 1000$. We used the SV (single vessel) fractionation factor between CO_2 and $CaCO_3$ of Swart et al. (1991).

Paleomagnetic Sampling and Analytical Methods

Previous magnetostratigraphic calibration of the Rohtas strata was based on preliminary work by Opdyke et al. (1979) that focused on the upper part of the sequence, with about one sample site per 30 m. In order to extend the magnetostratigraphic calibration into older strata and provide a stronger basis for correlation with the GRTS, J. Kappelman, J. Hicks, and I.A. Khan resampled the Rohtas section at higher resolution (average of one sample site per 10.8 m). Rock samples were collected from 314 sites with either a hand rasp (following the procedure outlined by Johnson et al., 1975) or a Pomeroy water-cooled gasoline drill. At least three samples were collected from each site within a vertical interval ranging from 0.1 to 0.5 m and a lateral distance generally <1 m. Each core was drilled to a depth of 7 to10 cm in order to avoid the outer weathered rock surface. Measurements were made on a 2G SCT superconducting magnetometer in a magnetically shielded room at the University of Texas. For further information on sampling and laboratory procedures, see Data Repository item part 1 (see footnote 1).

Previous studies of Siwalik sediments have shown that both magnetite (Opdyke et al., 1979) and specular hematite (Tauxe et al., 1980) can serve as the carriers of the primary magnetic remanence. It is common to find varying contributions of pigmentary hematite in these rocks as well (Tauxe et al., 1980, Tauxe and Badgley, 1984; Stubblefield, 1993). Given this potential mix of magnetic minerals, thermal demagnetization is preferred over alternating-field

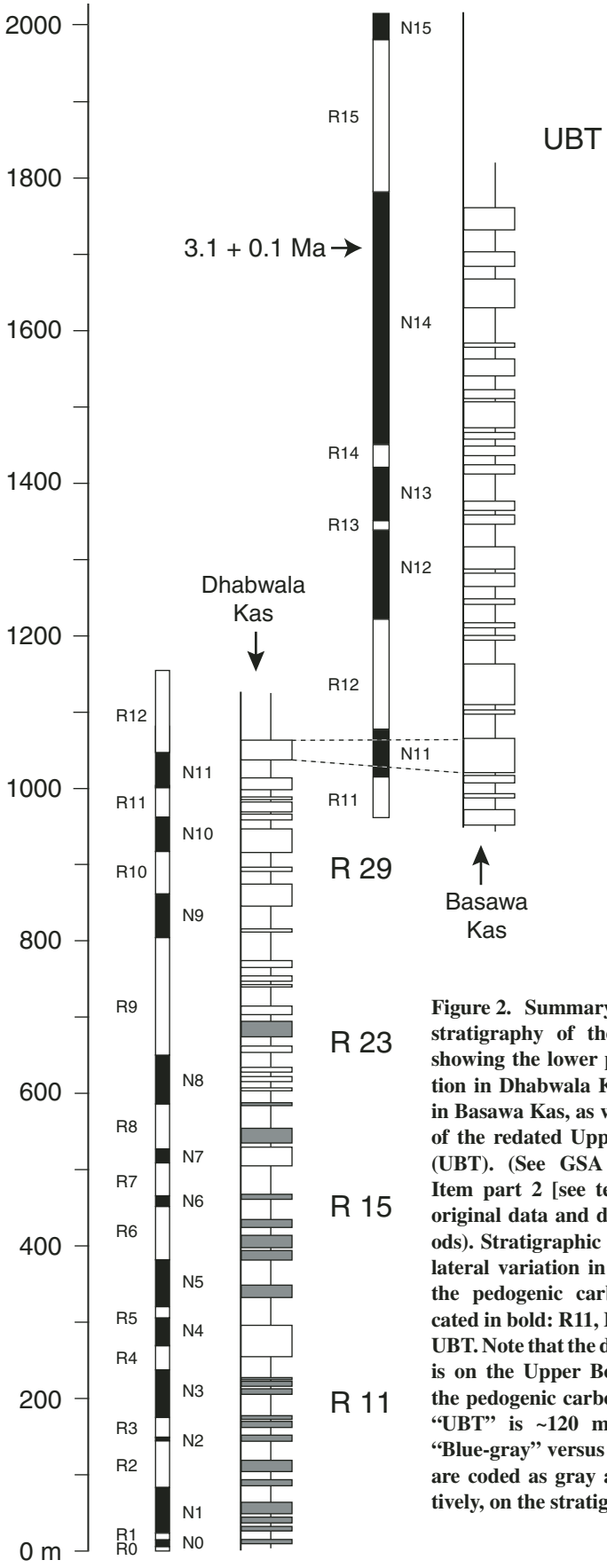

Figure 2. Summary of the reversal stratigraphy of the Rohtas section, showing the lower portion of the section in Dhabwala Kas and the upper in Basawa Kas, as well as the position of the redated Upper Boundary Tuff (UBT). (See GSA Data Repository Item part 2 [see text footnote 1] for original data and discussion of methods). Stratigraphic levels sampled for lateral variation in stable isotopes in the pedogenic carbonates are indicated in bold: R11, R15, R23, R29 and UBT. Note that the date of 3.1 ± 0.1 Ma is on the Upper Boundary Tuff, but the pedogenic carbonate level labeled "UBT" is ~120 m above this tuff. "Blue-gray" versus "buff" sandstones are coded as gray and white, respectively, on the stratigraphic column.

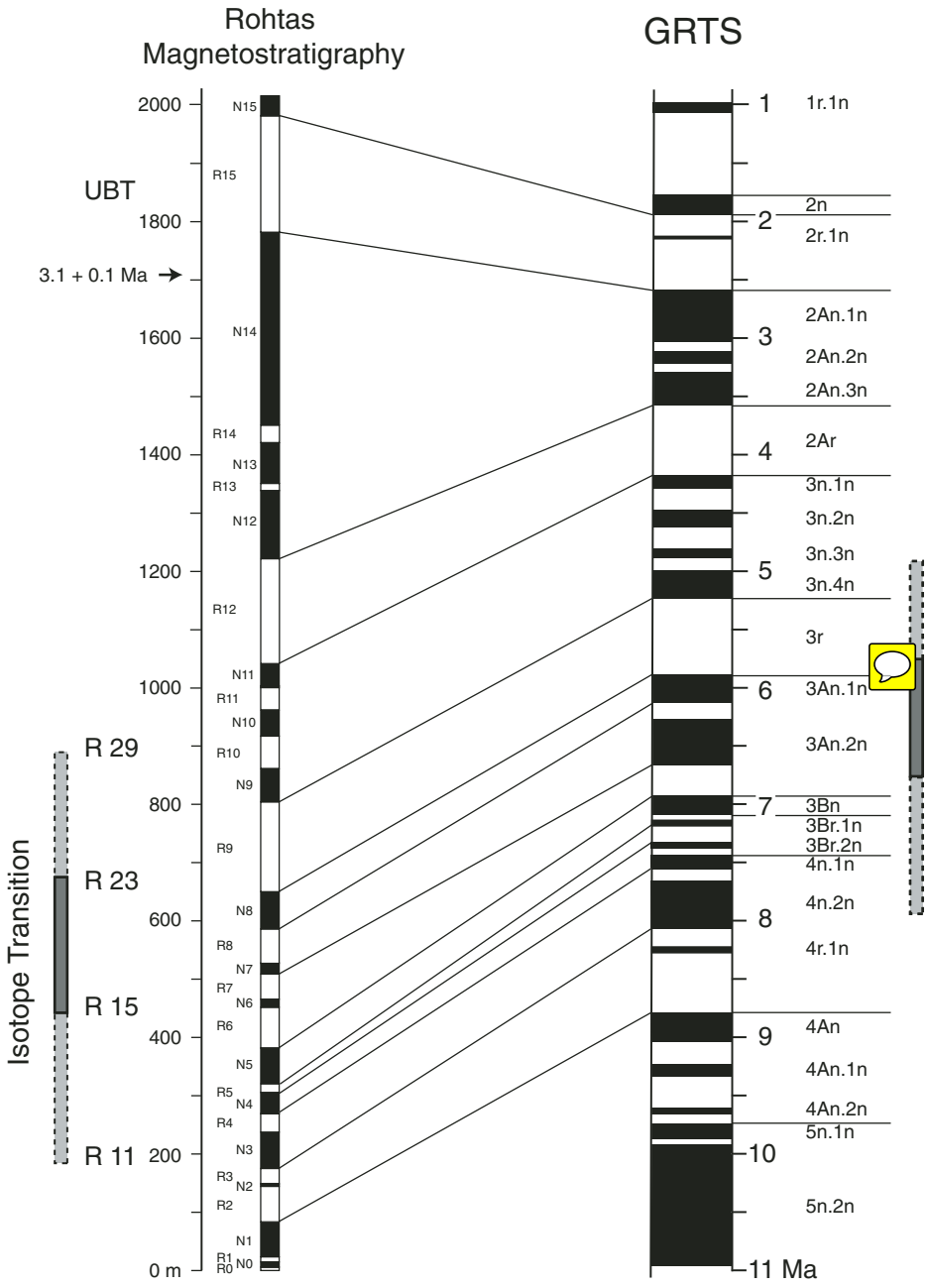

Figure 3. Reversal stratigraphy of the Rohtas section correlated to the geomagnetic reversal time scale (GRTS) (Cande and Kent, 1995). The long, dominantly normal zone in the upper portion of the Rohtas section is correlated to Chron 2An; the middle, dominantly reversed zone to Chrons 2Ar to 3r; and the lower, dominantly normal zone to Chrons 3Bn to 4An (Data Repository item part 1, Fig. DR5 [see text footnote 1]). The Siwalik C_3-C_4 transition as defined by Quade et al. (1989a) ($\delta^{13}C$ [Peedee belemnite] values of –9.0 or higher) is first evident at the 200 m level (7.9–8.1 Ma) and is essentially complete above the 900 m level (i.e., above ca. 5.0 Ma), although local patches of C_3 vegetation persisted until at least 4.85 Ma in several fluvial sub-environments (see text and Fig. 7). Solid portions of vertical bars next to the columns indicate the major interval of transition from C_3 to C_4 dominated vegetation.

(AF) demagnetization. A program of step-wise thermal demagnetization was used to remove secondary magnetic components acquired from either the present or past fields or oxidation reactions. Temperature stepping (7–10 steps/sample) was carried out with a low-field Schonstedt Thermal Demagnetizer (TSD-1) in a shielded room. Calculations were made using PaleoMagCalc©, a paleomagnetic analysis program for Windows (Crowe et al., 1993).

Values were accepted as statistically significant if the maximum angular deviation (MAD) value was less than 15°. In those cases where the MAD value exceeded 15° but the polarity of the sample was not in question, a mean vector was calculated using the various temperature steps with Fisher (1953) statistics, and statistical significance was evaluated with Watson's (1956) test for randomness. Site means and virtual geomagnetic pole latitudes were next calculated using Fisher statistics for those sites with three or more statistically significant samples. Statistical significance was again tested with the Watson (1956) criteria.

RESULTS AND DISCUSSION

Paleomagnetic Dating

Results from the 314 sample sites reveal a mixture of normal and reversed polarities (Figs. 3 and 4; see also Data Repository item part 1 [see footnote 1]), with a long, dominantly normal zone of nearly 600 m (N12–N14) in the upper portion of the section, and a long, dominantly reversed zone of over 800 m (R6–R12) in the lower half of the section that includes many shorter intervals of normal polarity of varying duration (N6–N11). Most of the polarity intervals are defined by multiple, statistically significant sites. Five intervals (R0, R1; N0, N2, N15) are defined by a single significant site, but these are generally constrained by closely spaced sites of opposite polarity, suggesting that these intervals are well defined.

The lower (Dhabwala Kas) and upper sections (Basawa Kas) at Rohtas are separated from one another along strike by ~1 km (Fig. 1) and have a composite thickness of 2020 m. Both sections were sampled for overlap (Fig. 2; Data Repository item part 1, Fig. DR3), and the results show that polarity zones R11-N11-R12 are present in both sections. The correlation between the two sections is supported by tracing the stratigraphic level of the Rohtas–Jogi Tilla Road (Fig. 1), which follows the strike of the sandstone beds. The Siwalik C_3-C_4 transition as defined by Quade and Cerling (1995) ($\delta^{13}C$ [PDB] values >–9.0) is first recorded at Rohtas in the 200 m level (R11: 8.0 Ma). $\delta^{13}C$ values

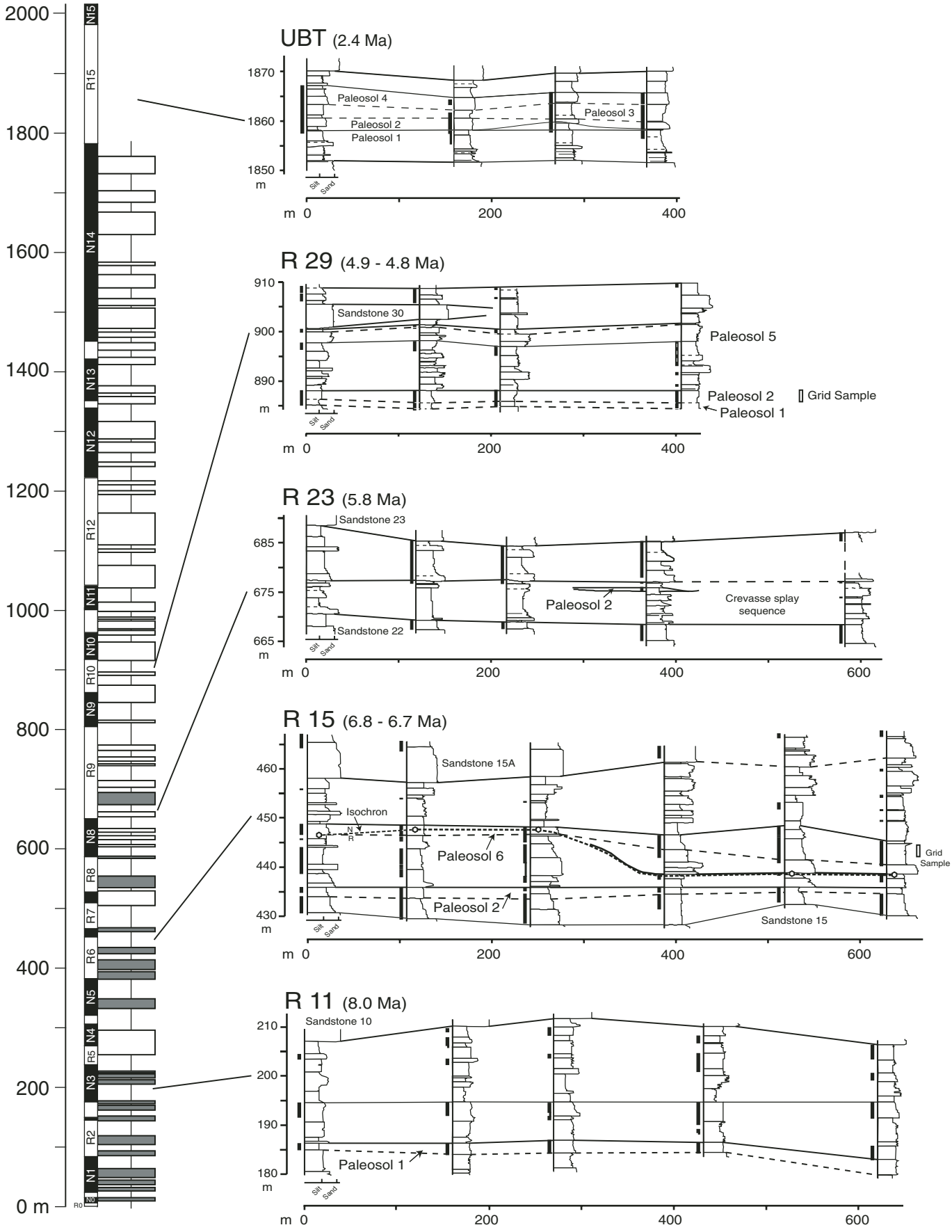
2000
1800
1600
1400
1200
1000
800
600
400
200
0 m
N15
R15
N14
N13
R12
N12
N11
N10
R10
N9
R9
N8
R8
R7
R6
N5
N4
R5
N3
R2
N1
N0
R0
UBT (2.4 Ma)
1870
1860
1850
m
Paleosol 4
Paleosol 2
Paleosol 1
Paleosol 3
Silt
Sand
m 0
200
400
R 29 (4.9 - 4.8 Ma)
910
900
890
m
Sandstone 30
Paleosol 5
Paleosol 2
Paleosol 1
Grid Sample
m 0
200
400
R 23 (5.8 Ma)
Sandstone 23
685
675
665
m
Paleosol 2
Crevasse splay sequence
Sandstone 22
m 0
200
400
600
R 15 (6.8 - 6.7 Ma)
460
450
440
430
m
Sandstone 15A
Isochron
N
R
Paleosol 6
Paleosol 2
Grid Sample
Sandstone 15
m 0
200
400
600
R 11 (8.0 Ma)
210
200
190
180
m
Sandstone 10
Paleosol 1
m 0
200
400
600

Figure 4. Rohtas magnetostratigraphic and lithostratigraphic column with the five laterally sampled panels, showing the measured sections and correlations of the major lithological units. "Blue-gray" versus "buff" sandstones are coded as gray and white, respectively, on the stratigraphic column. Intervals leached of matrix carbonate are indicated by the black bars to the left of each measured section; these generally coincide with the laterally traceable paleosols. Circles and fine dashed line on the R15 panel show the position of the paleomagnetic isochron (R6 to N6 on Fig. 3). All panels are plotted to the same horizontal and vertical scale. Numbers to the left of each panel give the meters above the base of the composite Rohtas section. Note: For reasons of space, only part of the actual lateral extent of R15 Psol 2 is shown in the diagram; also, continuous lithological description goes up to 1800 m; paleomagnetic log covers the entire 2020 m.

transitional between –9 and –2‰ are evident at both the R15 (450 m) and R23 (670 m) levels (solid and dashed bars in Fig. 3). The R23 level can be securely placed near the base of C3r of the geomagnetic reversal time scale (GRTS) at 5.86 Ma. The R15 level straddles a magnetic polarity shift that dates to 6.75 Ma if R6-R7 correlates to 3An.2r (Cande and Kent, 1995) (Fig. 3). An alternative correlation of Rohtas N6 to C3Br.1n yields an interpolated date of 7.17 Ma. We prefer the first correlation because it supports a relatively constant depositional rate throughout the Rohtas sequence (0.28 mm/yr; Data Repository item part 1, Fig. DR5), although this also requires one normal event of ~90 k.y. duration (N6) which is not recorded in 3An.2r of the GRTS. The preferred correlation requires slightly faster deposition during R6–R7 and slower deposition or erosion in N7–R8, relative to the average rates in the lower 1100 m of the Rohtas sequence (Fig. 3; GSA Repository item part 1). The Siwalik C_3-C_4 transition is regarded as complete (i.e., most $\delta^{13}C$ values >–2 ‰) by the R29 level at 870 m (4.7 Ma).

Numerous thin volcanic tuffs are present in the upper part of the section; dates for some of these are given in Johnson et al. (1982b), Opdyke et al. (1979), and Johnson et al. (1979). We have redated one of these tuffs (upper boundary tuff or UBT) at the 1700 m level (composite section) at 3.1 ± 0.1 Ma ($^{40}Ar/^{39}Ar$ on biotite; Data Repository item part 1, Table DR3, Figs DR4-DR5), and this date helps to constrain correlation of the upper part of the section to the GRTS. It is apparent from Figure 3 that rates of sediment accumulation in the Rohtas area increased post-3.6 Ma, after remaining relatively constant at ~.21 mm/yr for the previous ~6.0 m.y.

An additional biostratigraphic datum, the Old World appearance of the perissodactyl *Hipparion,* indicates that the base of the Rohtas section postdates Chron 5 or 10.9 Ma because specimens of *Hipparion* occur near the base of this section. Determinations of the age of the *Hipparion* datum in the Miocene Sinap Formation of Turkey (Kappelman et al., 1991, 1996; Bernor et al., 2003) and recalibration of the first occurrence of this taxon in the Siwalik Group (Pilbeam et al., 1996; Barry et al., 2002) suggests that this event was largely synchronous and occurred near the beginning of the long normal of Chron 5 (but see Sen, 1989; Garcés et al., 1997). The time scale of Cande and Kent (1995) places this event at ca. 10.7 Ma in both Turkey and Pakistan. Furthermore, the absence of a distinctive long normally magnetized zone at the base of the Rohtas section indicates that this interval postdates the end of Chron 5 at 9.92 Ma.

Our correlation to the GRTS (Fig. 3) differs from that of Opdyke et al. (1979) primarily because this earlier study relied on a coarser sampling density that missed many of the short normal and reversed intervals identified in the present study. In addition, Opdyke et al. (1979) relied on AF demagnetization, and this laboratory protocol was probably not sufficient to remove the stubborn normal overprint present in many samples (Data Repository item part 1; see footnote 1).

Siwalik Paleosols

Previous work on Siwalik paleosols focused on their relationship to fluvial lithofacies and architecture and comparisons with modern alluvial soils. In India, Nagri Formation paleosols were initially characterized as immature oxisols whose degree of development and internal features were controlled primarily by proximity to active channels (Johnson, 1977; Johnson et al., 1981). Johnson et al. (1981) identified paleosols of the Dhok Pathan Formation of the eastern Potwar as semiarid alphasols and noted

TABLE 1. AVERAGE CARBON AND OXYGEN ISOTOPE VALUES FOR EACH OF THE PALEOSOLS USED FOR LATERAL ANALYSIS IN THE ROHTAS AREA

Paleosol	N	Level* (m)	Dist.† (m)	$\delta^{13}C$ (PDB)		$\delta^{18}O$ (PDB)		Facies and Soil Color	Age (Ma)§
				Average	S.D.	Average	S.D.		
R11 Psol 1	23	185	620	–10.01	0.82	–8.98	0.58	Floodplain (orange)	7.98
R15 Psol 2	13	436	1073	–4.00	0.98	–8.04	0.45	Floodplain (red)	6.78
R15 Psol 6	28	448	730	–6.85	2.50	–8.18	0.93	Combination FP, CF	6.74
R15 Psol 6 FP**	14	448	400	–5.83	2.95	–7.73	0.88	Floodplain (yellow)	6.74
R15 Psol 6 CF	14	448	330	–7.87	1.44	–8.64	0.76	Channel fill (yellow-brown)	6.74
R23 Psol 2	13	676	89	–7.67	2.74	–8.85	1.10	Crevasse Splay (red)	5.78
R29 Psol 1	4	886	315	0.43	1.10	–7.03	0.63	Floodplain (red)	4.86
R29 Psol 2	6	888	315	–1.23	2.25	–7.04	1.25	Floodplain (yellow-brown)	4.85
R29 Psol 5	3	901	315	–2.92	0.62	–8.17	0.61	Crevasse splay (red)	4.78
UBT Psol 3	4	1860	270	2.86	0.66	–6.63	0.13	Floodplain (brown)	2.42
UBT Psols 1–4	9	1850–62	270	2.21	0.83	–6.06	0.90	Floodplain (brown)	2.42
R15 Grid	15	448	3.2	–8.59	0.62	–8.96	1.03	Floodplain (yellow-brown)	6.74
R29 Grid	15	888	1.2	–1.55	1.86	–6.65	0.36	Floodplain (yellow-brown)	4.85

Note: PDB—Peedee belemnite; S.D.—standard deviation; UBT—upper boundary tuft.

*Stratigraphic level is for the top of the paleosol above the base of the section. The level of UBT Psol 3 is based on lateral correlation to the measured magnetostratigraphic column, with a possible error of +20 m.

†Distance = total lateral extent of sampling for each paleosol (not the total extent of the paleosol).

§Age is based on paleomagnetic data presented in Figure 4 (See also GSA Data Repository part 2; see text footnote 1).

**FP = Floodplain (0–370 m on x-axis, Fig. 10) and CF = Channel fill (370-770+ m on x-axis, Fig. 10)

a trend toward increasing aridity through the Mio-Pliocene. Further work on two restricted stratigraphic intervals (58 m thick at ca. 9.4 Ma and 38 m thick at ca. 8.6 Ma) in the Khaur area ~130 km northwest of Rohtas identified nine soil types based on thickness, parent material, and degree of soil development (Retallack, 1991). Retallack (1991) interpreted the suite of paleosols from the Dhok Pathan Formation as representing seasonally wet to dry tropical climates that supported both forests and grasslands.

Three major lithofacies compose the fluvial architecture of Siwalik Group deposits: stratified sandstone, horizontally stratified mudstone (sandy silt to silty clay grade), and unstratified (massive) sandstones and mudstones (sandy to silty clay). The first two of these facies represent primary sedimentation in major and minor channels and crevasse-splay lobes with finer-grained flood-basin deposits that built up the floodplains (Behrensmeyer et al., 1995). The third facies represents pedogenic modification of the primary deposits when they were exposed on temporarily stable alluvial land surfaces. Paleosols are distinguished on the basis of an overall massive (i.e., unstratified) appearance in outcrop, color, and internal features including homogenized (bioturbated) texture, ped structure, clay skins and slickensides, mottling, root/burrow traces, and dispersed to clustered pedogenic nodules ($CaCO_3$ and Fe-Mn-oxides) (Fig. 5). Paleomagnetic calibration indicates that the Rohtas paleosols represent intervals of 10^2–10^4 yr of pedogenesis, when deposition was slow to negligible on portions of the aggrading alluvial plain.

Paleosols in the Rohtas sequence occur in channel fill, crevasse-splay, and floodplain paleoenvironmental settings, which are recognized on the basis of lateral and vertical relationships of the paleosols with adjacent strata (Fig. 4). Channel-fill paleosols occur above channel deposits of varying scale and often fine upward through several meters of superimposed, silty to clayey pedogenically modified units that formed during gradual filling of the topographic depression left by the abandoned channel. Crevasse-splay paleosols are thin (<1 m), leached silty-clay units found within sequences of bedded, unleached (i.e., matrix $CaCO_3$ present) sands, silts, and clays, which represent rapid vertical aggradation of crevasse-splay lobes on the Siwalik floodplains. Floodplain paleosols are the most laterally extensive and consistent in internal features; they typically cap decimeters to meters of unleached bedded sediments that represent coalesced, fine-grained splay deposits (Willis and Behrensmeyer 1994; Behrensmeyer et al., 1995; Khan et al., 1997; Zaleha, 1997). Internal features of paleosols in these three contexts are similar, although there tends to be more pedogenic carbonate, mottling, and clay cutan development in floodplain soils compared with channel-fill and crevasse-splay soils.

Many paleosols in the Siwalik deposits have pedogenic carbonate in the form of dispersed, irregular to roughly spherical nodules 0.5–2.0 cm in diameter (carbonate Stage II of Gile et al., 1966) (Figs. 5F and 5H). These commonly are concentrated 0.3–0.5 m below the upper contacts of paleosols that range from 1.0–3.0 m thick and are associated with other pedogenic features typical of B horizons including illuviated clay, mottling, root-burrow traces, and Fe-Mn hydroxide nodules. The carbonate nodules formed by plant-generated soil CO_2 interacting with matrix calcium during cycles of soil wetting and drying. Dispersed calcium carbonate is a pervasive matrix component typically forming a small proportion (3%–15%) of the Siwalik silt-grade sediments throughout the Rohtas and other Siwalik stratigraphic sequences (Quade and Cerling, 1995; Quade and Roe, 1999). This matrix carbonate was leached during pedogenesis and contributed to the formation of soil carbonate nodules (see later section on detrital contamination of the isotope values). Varying concentrations of pedogenic carbonate nodules in different Siwalik paleosols likely reflect local differences in chemical conditions affecting carbonate precipitation, and perhaps also short-term shifts in rainfall and temperature over 10^2-10^4 yr. Lateral variation in pedogenic features within individual paleosols has been attributed to variable substrate texture and drainage, which are controlled by channel proximity and floodplain topography (Johnson, 1977; Johnson et al., 1981; Retallack, 1991; Behrensmeyer et al., 1995; Willis and Behrensmeyer, 1994, 1995). Since $CaCO_3$ nodules precipitate at solution pH above ~7.0, while hydroxide minerals in Fe-Mn nodules (e.g., goethite) generally form at lower (or much higher) pH (Schwertmann and Murad, 1983), the co-occurrence of these precipitates indicates that chemical conditions within the soils shifted between reducing and oxidizing, perhaps seasonally or over longer periods during the lifetime of the soil. Both $CaCO_3$ and Fe-Mn nodules occur in floodplain channel lags, evidence that they formed in zones of active pedogenesis and were available for penecontemporaneous reworking.

Through the Neogene, Siwalik paleosols change in color and in the preservation of A-horizons, but internal morphological features, including the presence of pedogenic carbonate, remain relatively consistent (though locally variable). The major change in the Rohtas paleosols involves the appearance of yellow soils (Munsell 10YR) at the 450 m level (R15), ca. 6.8 Ma (Figs. 2 and 5F); these soils continue through the transition to the buff fluvial system and are common throughout the remainder of the section. The yellow paleosols typically have increased preservation of organic carbon relative to contemporaneous orange paleosols. The same color and carbon preservation shift occurs at about the same time in Siwalik paleosols from Pakistan to Nepal (Quade et al., 1995) in sections with greatly differing thicknesses and therefore diagenetic histories. This pattern of increased preservation of organic carbon upward in the sequence may

Figure 5. Views of the Rohtas outcrops and lithologies used in this study. (A) The R11 paleosol (Section R11-3), an interval of red-orange pedogenically modified mudstones where the lower figure is standing, between light-red, bedded mudstones. (B) Close view of the R11 paleosol, showing $CaCO_3$ rhyzoliths and pedogenic nodules. (C) Close view of $CaCO_3$ rhyzolith in B (rectangle in A). (D) Fluvial strata above the channel fill at section R15-5 (See also Fig. 4, section at 400 m). (E) Detail of sampling trench for Psol 6 (where two figures are digging) at R15-5 (white box in D) and red Psol 2 above blue-gray sandstone to right. (F) The first (lowest) yellow paleosol in the R15 level (Section R15-1, Psol 2.5 [J. Quade for scale]); note abundant $CaCO_3$ pedogenic nodules eroding from the B horizon. (G) R15-Psol 6 level showing grid sample site, with J. Hicks for scale (See also Fig. 9). (H) Detail of paleosol in G, showing pedogenic dark brown, spherical limonitic nodules with red weathering halos and irregular carbonate nodules (arrows). (I) Dark red, crevasse-splay paleosol (arrow) at the R23 level (Section R23-4S1), with a more typical yellow paleosol in the background; sandstone R23 near the top of the photo. (J) R29-Psol 2 grid sample (Section R29-1); Imran Khan for scale (see also Fig. 9). (K) Crevasse splay red paleosol (arrow) R29-Psol 5 (Section R29-4), within bedded mudstones, underlying a major channel sandstone. (L) Dark gray-brown R29-Psol 2, showing underlying marl and overlying bedded mudstones (Section R29-5); Jacob's staff is 1.8 m. (M) Succession of gray, brown, and yellow-brown paleosols at the UBT level, below a buff channel sandstone (J. Quade in lower part of photo for scale).

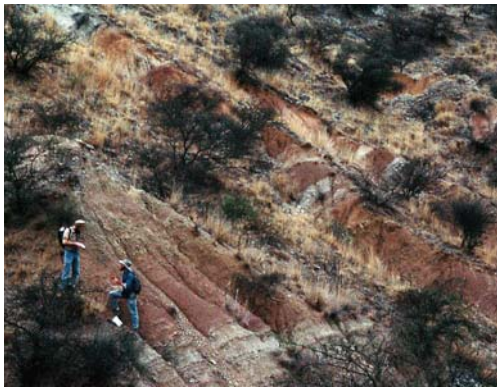


B


C


D


E


F


G

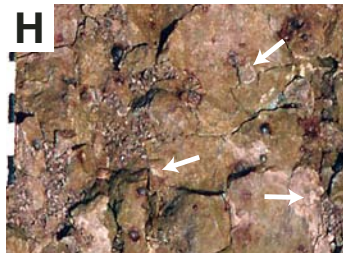
H


I

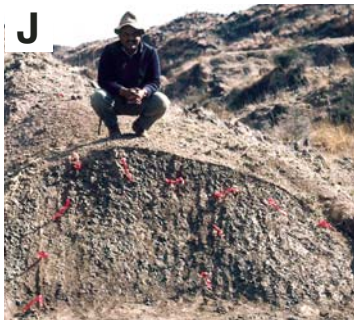
J

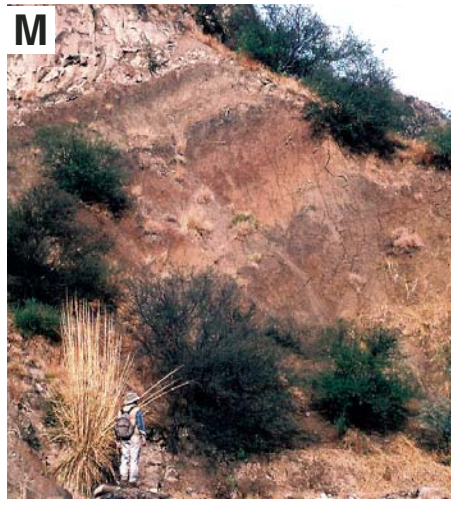
M


K


L

reflect vegetation and climate change that promoted more well-developed humic A horizons (e.g., grasslands) (Quade and Cerling, 1995). Although the appearance of the yellow paleosols occurs within the transition from blue-gray to buff fluvial systems in the Rohtas sequence, these paleosols appear within both the blue-gray and buff systems at 7.0–6.0 Ma elsewhere in the Pakistan Siwaliks. Thus, both isotopic and color changes through time in the paleosols appear to be independent of the different (i.e., blue-gray versus buff) fluvial systems.

Carbon Isotope Results and Discussion

The Carbon Isotope System

The stable carbon isotopic composition of paleosol organic matter or carbonate can be used to reconstruct aspects of vegetation present during soil formation (Cerling, 1984; Cerling et al., 1989). In modern-day Pakistan, all trees, most shrubs, and winter grasses are C_3 plants. Most grasses in Pakistan grow during the summer monsoon and are C_4 plants. $\delta^{13}C$ (PDB) values of modern C_3 and C_4 plants from East Africa (Cerling et al., 2003) average −25.5 ± 1.3‰ and −11.8 ± 1.4‰, after correction for the ~1.5‰ post-industrial shift in the $\delta^{13}C$ value of atmospheric CO_2.

Studies of modern soils (Cerling, 1984; Cerling et al., 1989; Quade et al., 1989b) indicate that the $\delta^{13}C$ values of coexisting organic matter and carbonate in soils are directly linked where respiration rates are high. As plants respire and decay, they respire soil CO_2 with a carbon isotopic composition directly reflecting the relative proportion of C_4 to C_3 plants growing on the soil. The ^{13}C in this soil CO_2 diffuses more slowly than ^{12}C, thus kinetically enriching soil CO_2 in contact with soil water by 4.2–4.4‰ (Davidson, 1995). Calcium carbonate will be a further 9–11‰ (depending on temperature) enriched in ^{13}C in the course of open-system, equilibrium exchange with the already kinetically enriched CO_2 diffusing upward through the soil (Cerling et al., 1989; Quade et al., 1989b). As a result, deep (>50 cm) in most soils outside of deserts, the isotopic composition of soil carbonate should differ from that of coexisting plant cover by ~13–15‰. Thus, soil carbonate formed in the presence of end-member C_3 and C_4 vegetation will have $\delta^{13}C$ values of −10.5 ± 2 and +2.7 ± 2‰, respectively. Higher in the soil profile, soil CO_2 will begin to mix with atmospheric CO_2, the exact depth depending on local soil respiration rates and the pCO_2 of the atmosphere. For this reason, our carbonate sampling depths below the tops of paleosols generally exceeded 50 cm. In this and our previous plant reconstructions for Pakistan, we assume that soil respiration rates were sufficiently high and atmospheric pCO_2 low enough (Pagani et al., 1999) that atmospheric CO_2 did not influence the $\delta^{13}C$ value of soil carbonate. The assumption of high respiration rates—as well as of open-system exchange between carbon species—is justified by the 13–15‰ separation, both predicted by the model and observed between $\delta^{13}C$ values in coexisting soil carbonate and soil organic matter in Siwalik paleosols (Quade et al., 1989a; Quade and Cerling, 1995; Davidson, 1995).

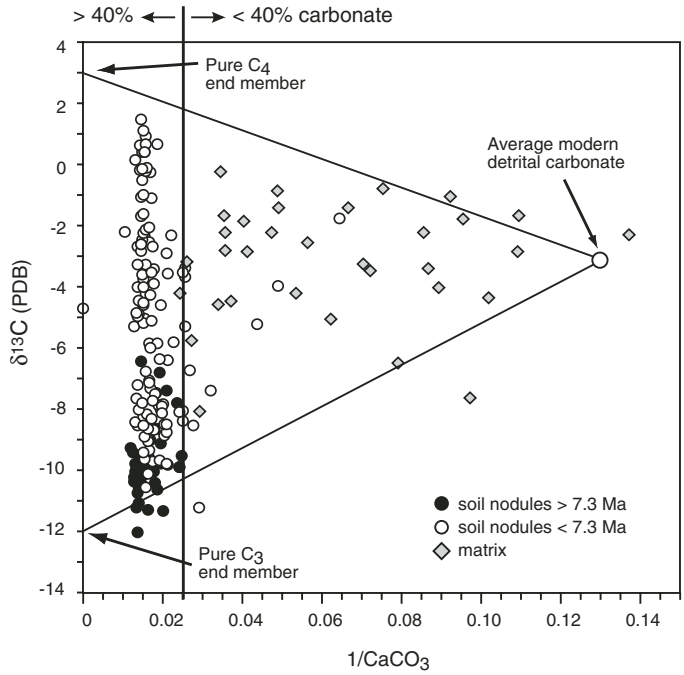

Figure 6. A mixing diagram with $\delta^{13}C$ values of carbonates versus $1/CaCO_3$ (in 1/%). The two endmembers potentially represented in any isotopic measurement of carbonates from the Siwalik Group are (1) detrital or "matrix" carbonate with very low percent carbonate and average $\delta^{13}C$ (Peedee belemnite [PDB]) values of −2.9 ± 1.1‰ (see Quade and Roe, 1999, for discussion and data sources); and (2) soil nodules with generally high (>40) percent carbonate and variable $\delta^{13}C$ values of −12 to +2‰, depending on the type of plant cover present during nodule formation. Any isotopic analysis used for paleovegetation reconstruction was rejected if the percent carbonate was <40, since these values would be moderately to strongly influenced by matrix carbonate contamination. Solid diagonal mixing lines define the field for predicted values of soil carbonate mixed with matrix carbonate.

Parent Material and Detrital Contamination of Paleosol Nodules

Detrital carbonate is present in low percentages (typically 3%–15%) in the unweathered, fine-grained clastic sediments of the Siwalik Group overbank deposits, potentially contaminating primary, plant-related soil carbonate (Quade and Cerling, 1995; Quade and Roe, 1999). Soil nodules contain a variable percentage of $CaCO_3$, in general >60% (Data Repository item part 2, Table DR4; see footnote 1). Most, if not all, of this carbonate is likely pedogenic, given the low percentage of $CaCO_3$ in parent material and the considerable in-soil leaching that preceded and accompanied soil formation. The ranges of ($\delta^{13}C$ and $\delta^{18}O$ values) in detrital carbonate are distinct from soil carbonate (Quade and Cerling, 1995; Quade and Roe, 1999). Consideration of the possible effects of a detrital carbonate contamination (Fig. 6) shows that below a value of ~40% total carbonate, detrital contamination could shift bulk $\delta^{13}C$ values by 1–2‰ depending on the $\delta^{13}C$ and $\delta^{18}O$ value of the plant-related carbonate. We therefore only use the isotopic values from nodules where the percentage of $CaCO_3$ > 40 in our vegetation and climate reconstructions (Data Repository item part 2, Table DR4).

Changes in $\delta^{13}C$ values through Time

The carbon isotope shift in the Pakistan Siwaliks, archived in both soil carbonates (Quade et al., 1989a; Quade and Cerling, 1995), meteoric calcite cements (Quade and Roe, 1999), and tooth enamel (Nelson, 2007), is reflected in the larger data set of $\delta^{13}C$ values from the Rohtas section (Fig. 7A). Despite a wide spread of values at most levels, the increase in the means of $\delta^{13}C$ values is statistically significant (*t*-test, ≥95%) between all levels except the R15 (6.75 Ma) to R23 (5.78 Ma) interval (Table 1). Results from R11 (8.0 Ma) at the bottom of the section yield an average $\delta^{13}C$ value of −10.0‰, consistent with a cover of pure to nearly pure C_3 plants with a $\delta^{13}C$ value of about −25‰. At the other extreme, results from the UBT (2.42 Ma) and ROT-104 (2.00 Ma) paleosol levels yield an average $\delta^{13}C$ value of +2.2‰, consistent with virtually pure C_4 grassland on the Siwalik floodplains. Standard deviations around the means of $\delta^{13}C$ values at the R11 and UBT–ROT-104 levels are low (0.62–0.82), showing that there was little variation in the floodplain vegetation from an isotopic perspective before or after the Siwalik C_3-C_4 transition.

In contrast, there is considerable variation in $\delta^{13}C$ values of carbonate during the main transition interval from ca. 7.0–5.0 Ma. Ranges and standard deviations of $\delta^{13}C$ values in sample populations are much higher (1.44–2.95) for most paleosols in the transition (R15, R23, R29) than below (R11) and above (UBT) (Table 1). Paleosols and their pedogenic carbonate are formed over hundreds to thousands of years (Machette, 1985) and may record substantial periods of time-averaging of short-term shifts in climate shifts vegetation ecotones. To explain the lateral variation in $\delta^{13}C$ values in the transition period between R15 and R29, we favor three possible scenarios (Fig. 8). Vegetation could have consisted of (A) stable patches of C_3 and C_4 plants at a spatial scale of hundreds of meters that did not migrate significantly during the time of soil formation; (B) patches of C_3 and C_4 plants at a spatial scale of hundreds of meters but unstable (i.e., they shifted around on the landscape) relative to the time of soil formation, at a spatial scale of hundreds of meters; or (C) an even, fine-scale (tens of meters) mix of C_3 and C_4 biomass. Scenerio (A) has been documented in soils supporting modern savanna and woodland habitats in Africa (Ambrose and Sikes, 1991) and India (Mariotti and Peterschmitt, 1994; Desjardins et al., 1996), testifying to the current instability of C_3-C_4 ecotones.

The spread of values on Figure 7A represents variation in C_3 versus C_4 vegetation within tightly constrained stratigraphic intervals as well as over long periods of time. In the following sections, we use a combination of detailed sedimentologic and isotopic information to examine how this variation correlates with local topography, substrate, and other features of successive fluvial paleolandscapes.

Small-Scale Variation in $\delta^{13}C$ Values

It is important to establish the range of isotopic variation within a few vertical and lateral meters in single paleosols in order to understand the potential effects of such local variation on larger-scale lateral patterns. For this we used measurements from pedogenic carbonates in two high-resolution "grid" samples from paleosol outcrops at the R15 and R29 levels (Table 1; Fig. 9).

The R15 grid sample was done on a two-dimensional, cleaned outcrop of a yellow-brown (Munsell 10YR 4-5/3-4) paleosol at the same stratigraphic level as Paleosol 6 but not directly traceable into it. This paleosol has consistent internal features throughout the sampled interval of 1.6 m (Figs. 5G, 5H, and 9A), which we interpret as evidence of an intensely bioturbated soil accumulated on an accretionary floodplain. The upper surface is truncated locally by a channel sandstone, so the original top of the soil was not available for sampling. The $\delta^{13}C$ values for 15 samples from an outcrop area of ~4.0 m^2 have a mean and standard deviation of −8.59 ± 0.62 (Table 1), and this standard deviation is small relative to $\delta^{13}C$

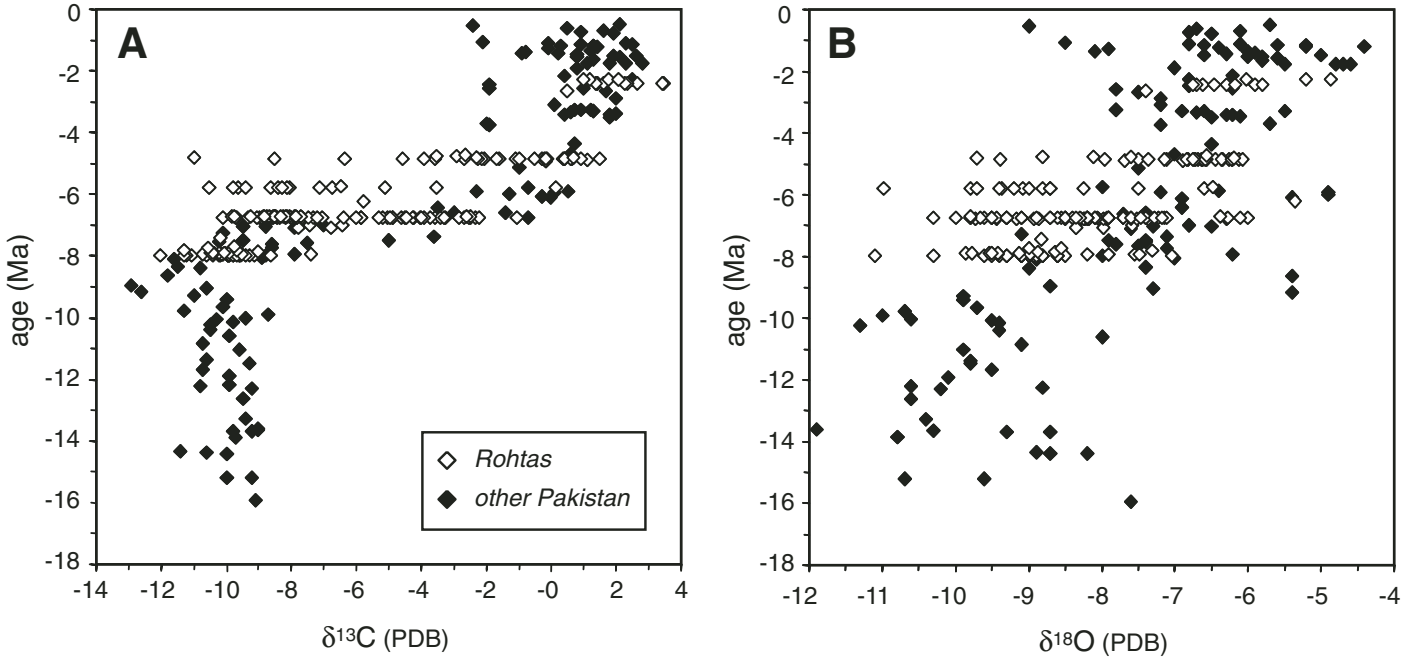

Figure 7. Trends with time for (A) $\delta^{13}C$ (PDB) and (B) $\delta^{18}O$ (Peedee belemnite [PDB]) values of carbonates from paleosols at Rohtas (open diamonds—lateral sampling of individual paleosols) and all other sections (solid diamonds—vertical sampling of successive paleosols) in the Siwalik Group of Pakistan (Quade and Cerling, 1995), using the timescale of Cande and Kent (1995). (Data Repository item part 3, Table DR7; see footnote 1).

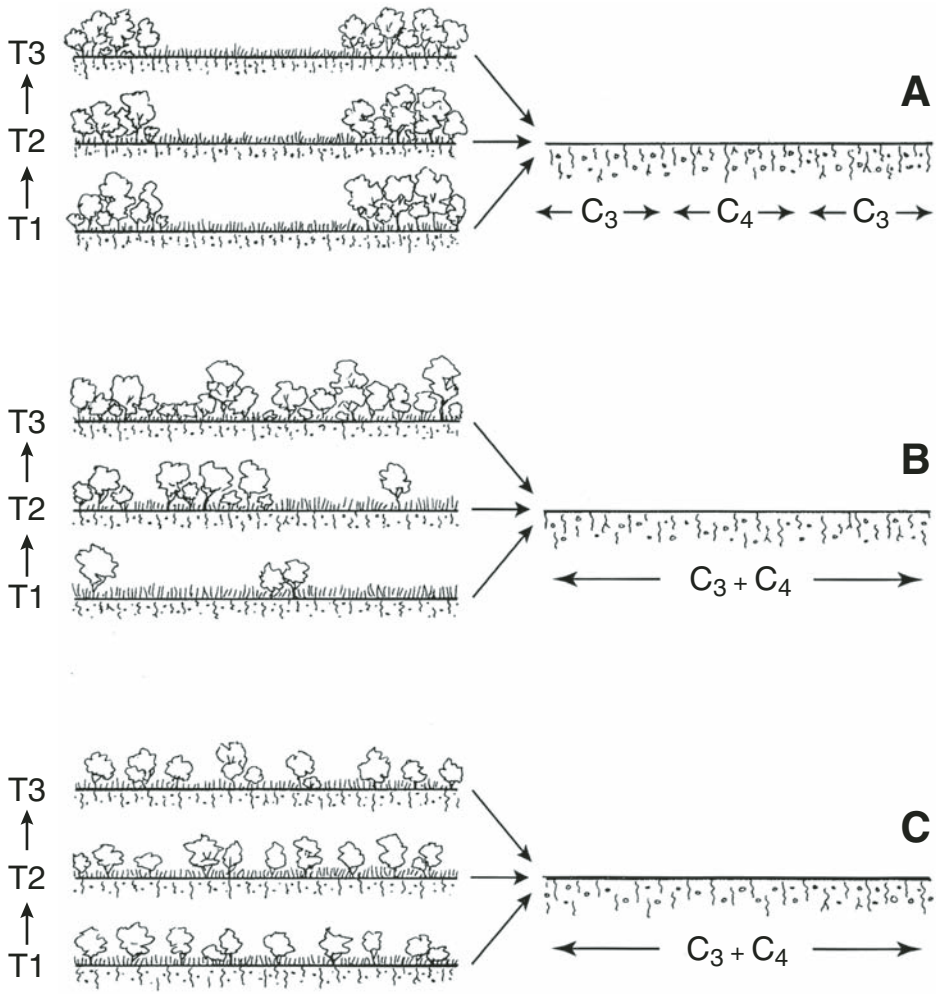

Figure 8. Three alternative models for vegetation patterns through successive time intervals (T1–T3) that could explain observed lateral variation in $\delta^{13}C$ (Peedee belemnite [PDB]) values in the pedogenic carbonates from Rohtas. On a spatial scale of hundreds of meters, vegetation may consist of (A) patches of C_3 and C_4 plants that remained stable during soil formation, resulting in distinct areas of lower and higher $\delta^{13}C$ values; (B) patches of C_3 and C_4 plants that shifted on the landscape during the time of soil formation, resulting in an intermediate $\delta^{13}C$ (PDB) value (possibly with high variability among different samples from the same paleosol); or (C) a persistent, evenly distributed, fine-scale (tens of meters) mix of C_3 and C_4 vegetation, also resulting in an intermediate $\delta^{13}C$ (PDB) value.

lateral variation (−6.85 ± 2.50) for paleosols within the R15 level. There is no indication of a systematic vertical shift in $\delta^{13}C$ values.

The second grid was sampled from Paleosol 2 at the R29 level (Figs. 5J and 9B). This paleosol is ~2.3 m thick and relatively homogeneous throughout, except for increased silt near the top, and is conformably overlain by bedded silts. It is yellow-brown with a distinct gray zone in the upper 10 cm, which likely is a preserved humic layer (A horizon). Paleosol 2 appears to be an accretionary floodplain soil that preserved some coarse primary bedding in spite of evidence for considerable bioturbation.

In contrast to the R15 paleosol, $\delta^{13}C$ values in R29 Paleosol 2 decrease upward through 2 m of soil thickness (Fig. 9B). We interpret this trend to result from a shift in the vegetation from dominantly C_4 to a mix of C_3 and C_4 (with one minor reversal) during the period of soil accretion and nodule formation The consistent change in the isotope values in three parallel vertical transects within the grid argues against significant vertical mixing of nodules due to bioturbation across the total time period spanned by the paleosol. This time interval would be ~6–8 k.y., the average maximum estimated duration of pedogenesis based on the total number of paleosols recorded through the R29 interval and paleomagnetic calibration (Data Repository Item part 1; see footnote 1). The isotope trends within R29 Paleosol 2 are similar in temporal scale to vegetation shifts recorded in soil organic matter in Holocene soils (Mariotti and Peterschmitt, 1994; Desjardins et al., 1996). Other investigations of isotopic values in pedogenic carbonates in late Pleistocene-Holocene soils that formed over similar time periods show that stratigraphic disordering can occur due to translocation of younger carbonate to deeper soil levels during wet climatic phases (Leamy and Rafter, 1972), but this would result in the reverse of the trend seen in R29-Psol 2 (i.e., C_4 above C_3 rather than an upward trend toward C_3).

Lateral Variation in Carbon Isotopes

Five stratigraphic panels covering lateral distances of 90–1100 m (Figs. 4 and 10; Table 1) provide the basis for examining $\delta^{13}C$ variation within individual Siwalik paleosols. All panels include a number of different paleosols as well as bedded overbank and channel deposits, and the overall architecture of the fluvial sediments is similar throughout except for the highest panel (UBT), which lacks major channel sands within the documented interval. We provide assessments of the lateral patterns in $\delta^{13}C$ and $\delta^{18}O$ values for each of our target levels, along with brief descriptions of macroscopic paleosol features and environmental context within the fluvial deposits.

R11-Psol 1 (8.0 Ma). R11-Psol 1 is the lowest paleosol in a sequence of floodplain strata underlying Sandstone 10 (Figs. 4, 5A–5C, and 10). It is laterally consistent in color (orange-brown; 10YR 5/4-5/6), texture, and internal features and is easily traceable over 620 m of exposure. In some areas, it has abundant, vertical, calcified rhizoliths up to 5 cm in diameter, with an upper zone of dispersed pedogenic carbonate nodules <1 cm in diameter overlying more abundant, larger nodules (a Bk horizon) (Figs. 5B and 5C). R11-Psol 1 overlies 4–5 m of unleached, finely bedded to homogenized (bioturbated) silts, which represent the typical fine-grained floodplain deposits of the Siwalik strata (Behrensmeyer et al., 1995). Based on the scale and frequency of the root traces and rhizoliths, this paleosol formed on a flat, emergent surface of a slowly aggrading floodplain and supported woody vegetation.

The $\delta^{13}C$ values for R11-Psol 1 average −10.0 ± 0.8 (Fig. 10; Table 1), which is consistent with a pure to nearly pure C_3 vegetation cover. The minor lateral variation in $\delta^{13}C$ values could result from differences in plant density, the $\delta^{13}C$ value of the C_3 plants themselves, or other factors. For example, the decrease in $\delta^{13}C$ values from

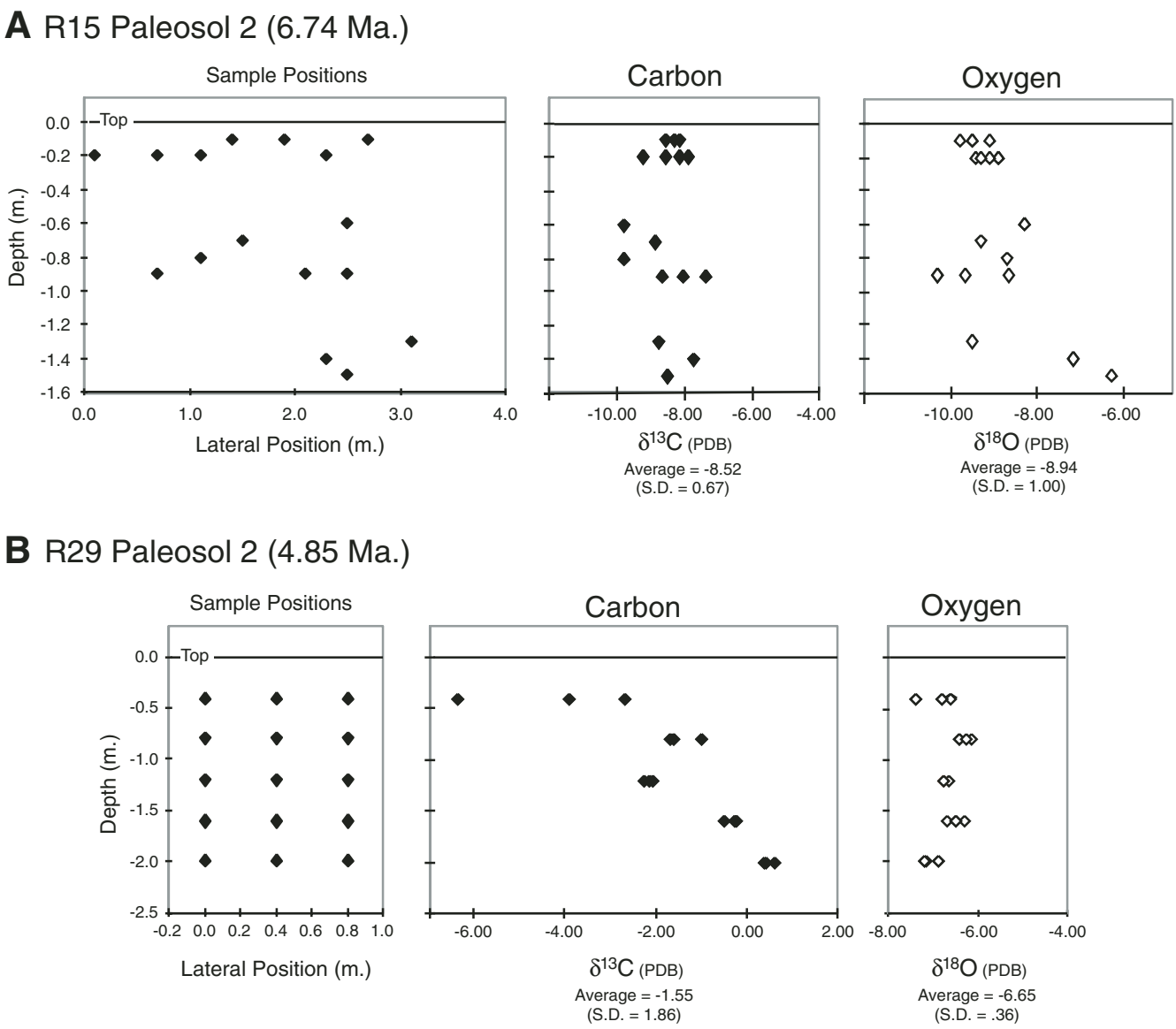

Figure 9. Grid samples of two different paleosols at the (A) R15 and (B) R29 levels showing small-scale lateral and vertical variation in $\delta^{13}C$ (Peedee belemnite [PDB]) and $\delta^{18}O$ (PDB) values. R29 Paleosol 2 shows a marked vertical increase in $\delta^{13}C$ values, indicating a shift from pure C_4 to a mix of C_3 and C_4 during the time of soil accretion.

southwest to northeast could reflect an increase in closed (forest?) vegetation in that direction (Codron et al., 2005). Overall, however, the lateral continuity of paleosol features in R11-Psol 1 corresponds to low variation in $\delta^{13}C$ values. Both soil morphologic and $\delta^{13}C$ values indicate a homogeneous, km-scale area of wooded landscape that was stable over the time of soil formation, which was <42 k.y. per soil based on paleomagnetic calibration (≤5 paleosols in 30 m representing a total of 211 k.y.).

R15-Psol 2 (6.78 Ma). R15-Psol 2 is a distinctively red paleosol (7.5YR 4/4-6 to 5YR 4/3-4) with abundant carbonate that can be traced laterally for over 1100 m. It formed on fine-grained, flat-lying floodplain deposits 3–7 m above a large buried paleochannel and is superimposed on an orange soil (5YR 5/6) at the top of the channel fill deposits of Sandstone 15 (Figs. 4, 5D–5E, and 10). Paleosol 2 has a silty to clayey texture and a distinctive Bk zone of linked, columnar $CaCO_3$ nodules. The density of pedogenic carbonate within Psol 2 is uneven, passing laterally from infrequent, dispersed nodules to abundant composite nodules. The soil is abundantly mottled with root and burrow traces, has well-developed cutans providing evidence for clay translocation, and sand-filled cracks indicating periods of desiccation. The $\delta^{13}C$ (PDB) values for R15-Psol 2 average –4.0 ± 1.0 (Table 1) and indicate mixed C_3-C_4 vegetation with 75% C_4; that is, a largely open, grassy area that was over 1 km in lateral extent. Four samples at 520 m (Fig. 10) with lower $\delta^{13}C$ values coincide with a break in the laterally persistent dense soil carbonate and could represent a persistent patch of trees. Psol 2 formed over a maximum of 15 k.y., based on paleomagnetic calibration. The high C_4 (grass) abundance contrasts markedly with C_3-dominated vegetation of the R11-Psol 1 (8.0 Ma). The R15 level represents the same time interval during which, in other Siwalik sections (Quade and Cerling, 1995), C_4 grasses were expanding. The C_4 vegetation implied by the results from R15-Psol 2

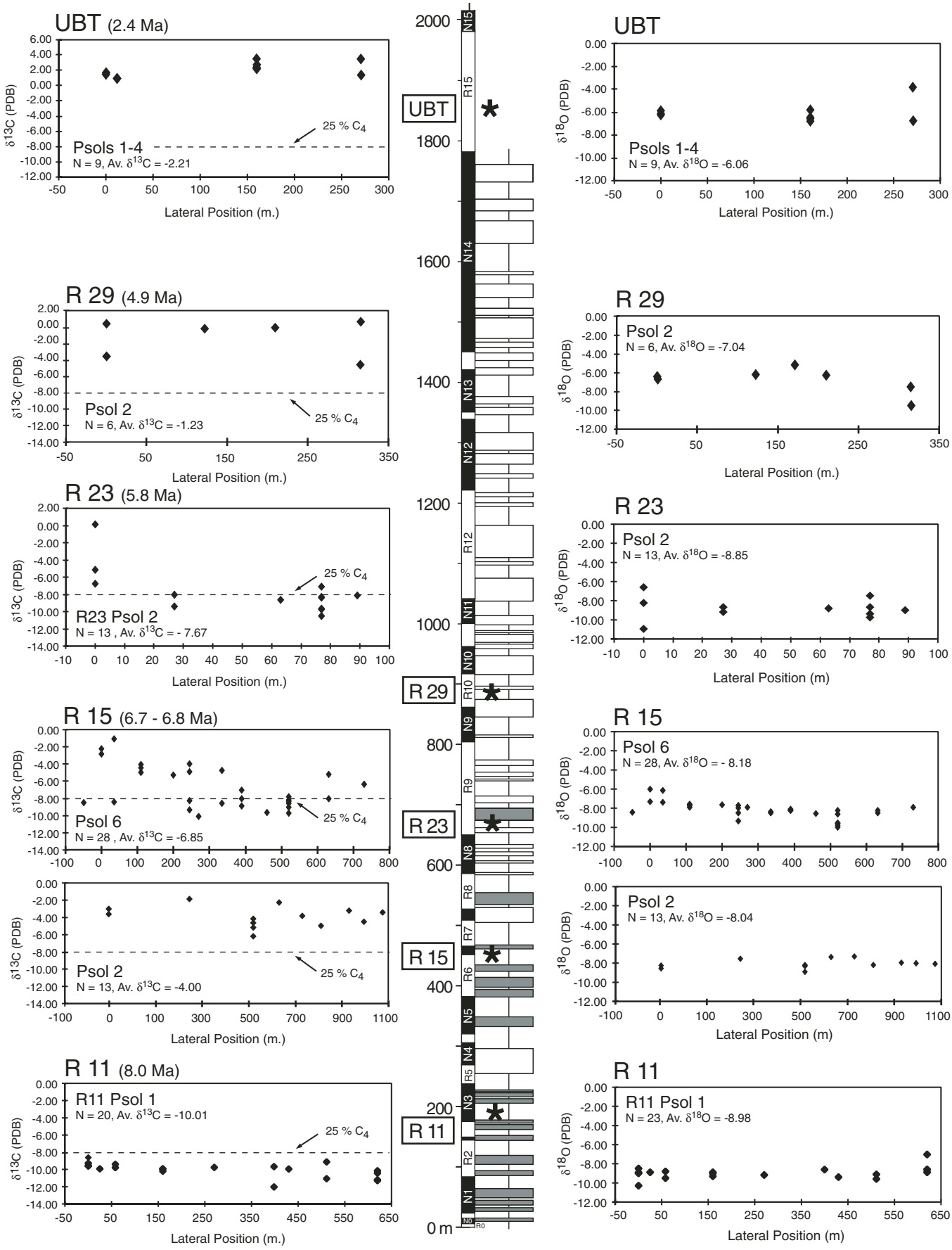
UBT (2.4 Ma)
Psols 1-4
N = 9, Av. δ13C = -2.21
25 % C4
δ13C (PDB)
Lateral Position (m.)
UBT
Psols 1-4
N = 9, Av. δ18O = -6.06
δ18O (PDB)
Lateral Position (m.)
R 29 (4.9 Ma)
Psol 2
N = 6, Av. δ13C = -1.23
25 % C4
Psol 2
N = 6, Av. δ18O = -7.04
R 23 (5.8 Ma)
R23 Psol 2
N = 13 , Av. δ13C = - 7.67
25 % C4
Psol 2
N = 13, Av. δ18O = -8.85
Lateral Position (m)
R 15 (6.7 - 6.8 Ma)
Psol 6
N = 28 , Av. δ13C = -6.85
25 % C4
Psol 6
N = 28, Av. δ18O = - 8.18
Psol 2
N = 13, Av. δ13C = -4.00
Psol 2
N = 13, Av. δ18O = -8.04
R 11 (8.0 Ma)
R11 Psol 1
N = 20, Av. δ13C = -10.01
R11 Psol 1
N = 23, Av. δ18O = -8.98
2000
1800
1600
1400
1200
1000
800
600
400
200
0 m
N15
R15
N14
N13
N12
R12
N11
N10
R10
N9
R9
N8
R8
R7
R6
N5
N4
R5
N3
R2
N1
N0
R0

Figure 10. Rohtas magnetostratigraphic column with plots of isotopic results for lateral samples of pedogenic carbonate, showing $\delta^{13}C$ (Peedee belemnite [PDB]) (left) and $\delta^{18}O$ (PDB) values values (right) within the target paleosols. In each diagram, the *x*-axis represents distance (meters) along strike, with SW to the left and NE to the right, and the *y*-axis shows the isotope values. Note that the *x*-axis scales vary for each level in the column, and the *y*-axis scales vary depending on the range of isotope results. Dashed line in $\delta^{13}C$ panels provides a reference representing about a maximum 25% C_4 (grass) component in the vegetation. The panels show the shift through time in the $\delta^{13}C$values but also stratigraphic mixing of C_3 versus C_4 vegetation, as well as both types of vegetation in the same paleosol (R15, Psol 6) during the Siwalik C_3-C_4 transition between 8.1 and ≤4.8 Ma. *Note:* for reasons of space, only part of the actual lateral extent of R15 Psol 2 is shown in the diagram (Table 1; see GSA Data Repository item part 2 [see text footnote 1]).

combined with the intensely oxidized red color, abundant soil carbonate, and desiccation cracking suggests that the soil was subject to intervals of strong seasonal wetting and drying.

R15-Psol 6 (6.74 Ma). R15- Psol 6 occurs ~15 m above Psol 2 in the R15 panel (Figs. 4, 5D–5H, and 10), and was selected for study because it is part of a package of the first strongly yellow-brown paleosols in the section, contrasting with the red to orange paleosols below this stratigraphic level. It is a yellow-brown silty-clay soil (10YR 4-5/3-4) with dispersed Fe-Mn nodules and a Bk horizon with $CaCO_3$ nodules (Fig. 5H). R15-Psol 6 can be traced for over 600 m from the southwest, where it is ~2 m thick and associated with flat-lying floodplain deposits toward the northeast, where it is up to 4 m thick and caps a channel fill deposit (Figs. 4, 5D–5H, and 10). Taking the underlying R15-Psol 2 as a horizontal, the upper surface of R15-Psol 6 dips slightly and becomes more topographically variable above the channel fill. Further evidence of the paleotopography is provided by a paleomagnetic polarity shift (R6-N6) evident within R15-Psol 6 (dashed line in Fig. 4). The normal zone (N6) at the top of the soil is thicker toward the southwest, thins toward the channel edge, then thickens abruptly in the channel, and the entire fine-grained channel fill is normal polarity. We infer that the active channel was contemporaneous with the formation of the lower part of R15-Psol 6. The channel then was abandoned and gradually filled with fine-grained silts and clays modified by pedogenesis, and these accretionary soils were contemporaneous with the upper part of the floodplain soil toward the southwest. Thus, the top of R15-Psol 6 represents a land surface that passed from floodplain to channel swale over the total sampled distance of ~600 m. The range of possible sampling error on the paleomagnetic boundary also implies a limit of ±0.3m on vertical mixing of pedogenic nodules in the soil by bioturbation during and after the polarity shift.

The $\delta^{13}C$ values R15-Psol 6 average −6.9 ± 2.5, indicating a mix of C_3 and C_4 vegetation (Table 1). There is a significant difference in population means (*t*-test, >95%), however, between the higher $\delta^{13}C$ values (-5.8 ± 3.0) in the floodplain context toward the southwest compared with lower $\delta^{13}C$ values (-7.9 ± 1.4) for the channel fill context toward the northeast (Fig. 10). The highest $\delta^{13}C$ values occur in the upper part of the paleosol, above the geomagnetic polarity shift, on the floodplain soil ~300 m from the edge of the contemporaneous channel swale. Although there are also a few lower $\delta^{13}C$ values in this context, most of the lower values occur in the channel-fill soil. We conclude that the paleovegetation varied from dominantly C_4 on the floodplain to the southwest to dominantly C_3 above the channel fill toward the northeast. This is consistent with trees and shrubs with long vertical tap-roots growing in the oxidized but relatively moist, silty to clayey substrate of an abandoned channel, while shallow-rooted grasses and forbs grew on the seasonally dry floodplain surfaces (e.g., Cole and Brown, 1976), which implies significant seasonal drought stress on the paleovegetation.

Studies of a modern savanna ecosystem indicate that that $\delta^{13}C$ values of C_3 plants can vary by 1%–2% per mil across different types of vegetation in fluvial environments, with the most depleted $\delta^{13}C$ values associated with seasonal riverbed and densely wooded riparian habitats (Codron et al., 2005). Based on comparisons with other habitats in the same ecosystem, these authors conclude that proximity to perennial water sources is the major control on relatively low C_3 plant $\delta^{13}C$ values, rather than canopy cover or local precipitation. The lateral variation of $\delta^{13}C$ values (−8.11 to −5.60) in Rohtas R15 Psol 6 thus could result not only from different proportions of C_4 versus C_3 vegetation, but also from lower $\delta^{13}C$ values associated with trees and shrubs in the channel swale environment.

R23-Psol 2 (5.78 Ma). This paleosol occurs in overbank silts and thin sands between Sandstones 22 and 23, ~200 m above the R15 level (Figs. 4, 5I, and 10). R23-Psol 2 is a relatively thin paleosol that lies within a 6–9-m-thick interval of well-bedded mudstones. It is light red-brown (7.5YR 4/2) with abundant blue-gray mottles and burrow fills, including a sand-filled spherical krotovina 13 cm in maximum diameter. The upper 40–60 cm is leached of matrix carbonate and contains abundant carbonate nodules but almost no Fe-Mn nodules. R23-Psol 2 can be traced for only ~90m laterally; to the northeast, it is truncated by a small channel, and toward the southwest, it separates into a complex of 10–15-cm-thick pedogenic zones alternating with bedded silts. From the overall sedimentary context (Fig. 4) and the microstratigraphic features of the adjacent units, we infer that R23-Psol 2 formed on a temporarily stable surface of a crevasse-splay lobe. It is thinner and less laterally extensive than the typical paleosols in the Rohtas section, but still bioturbated and leached.

Carbonate in R23-Psol 2 yielded uniform $\delta^{13}C$ values = −7.7 ± 2.7 (Table 1) as far as this paleosol can be traced with certainty (Fig. 4). These values contrast with laterally adjacent paleosols at the R23 level and are at odds with the previously determined $\delta^{13}C$ trend at 5.8 Ma (Fig. 7) (Quade and Cerling, 1995), which indicates dominant C_4 vegetation. Where R23-Psol 2 grades into a series of thinner paleosols to the southwest, the $\delta^{13}C$ values increase markedly, indicating dominantly C_4 grass cover (Fig. 10).

R29: Psols 1 (4.86 Ma) and 2 (4.85 Ma). R29-Psol 2 is a distinct, 1.5–2.5-m yellow-brown (10YR 4/2-2.5Y 4/2), nodule-rich unit that occurs immediately above R29-Psol 1, a separate red (5YR 4/4) soil with large single and composite carbonate nodules. Internal features remain consistent for at least 600 m laterally, and both soils formed in a floodplain context. R29-Psol 2 is conformably overlain by bedded to bioturbated, unleached silts, and sandy silts representing crevasse-splay deposition, which terminated pedogenesis. R29-Psol 1 is clay-rich, with abundant cutans, gray root traces and mottles, and abundant, columnar carbonate nodules, but, in contrast with the overlying soil, it lacks Fe-Mn nodules. Features of R29-Psol 2 were documented in detail at the site of the "grid" study (see earlier description) and at three additional sites along strike (Figs. 4, 5J, and 5L). The dispersed to clustered carbonate and Fe-Mn nodules as well as the clay cutans and mottles that occur in the lower portion of the profile of R29-Psol 2 decrease sharply in abundance in the upper 30 cm. This soil also coarsens upward from clay to sandy silt with a corresponding decrease in clay cutans, which we interpret as

evidence for clay translocation combined with an influx of slightly coarser sediment in the final stages of soil accretion.

The carbonate nodules sampled laterally in R29-Psol 1 yield an average $\delta^{13}C$ value of +0.4 ± 1.1, and in R29-Psol 2 an average $\delta^{13}C$ value of −1.2 ± 2.3 (Table 1), indicating dominantly C_4 vegetation at ~4.8 Ma, although the detailed grid analysis in Psol 2 indicates that there was a change from C_4 to increased C_3 plant cover over the lifetime of this soil (Fig. 8). Thus, although the Siwalik C_3-C_4 transition in southern Asia was essentially complete by 5.0 Ma (Quade et al., 1989a; Quade and Cerling, 1995), the detailed isotopic profile within R29-Psol 2 suggests continuing variability in vegetation, possibly driven by short-term climate shifts, that is obscured at coarser levels of sampling.

R29-Psol 5 (4.78 Ma). R29-Psol 5 occurs near the top of a 4–6-m-thick sequence of bedded fine sands and silts (Fig. 5K; Table 1), which represent crevasse-splay and levee facies similar to those associated with R23-Psol 2. These form a coarsening upward sequence above a mature floodplain paleosol (in this case, R29-Psol 4) that culminates in a channel sandstone. R29-Psol 5 is a thin (20–60 cm) but laterally persistent red (5YR 4/37–5YR 4/2), bioturbated, clayey silt, with small, dispersed carbonate nodules, mottles, root traces, abundant clay cutans, and no Fe-Mn nodules.

Three sample sites along the R29-Psol 5 provide an average $\delta^{13}C$ value of −2.9 ± 0.6, indicating dominantly C_4 vegetation on this soil at ca 4.8 Ma. This contrasts with the $\delta^{13}C$ values indicating dominant C_3 vegetation in a similar crevasse-splay soil at 5.8 Ma (R23-Psol 2), suggesting either that there was considerable variability in the plants that colonized these short-lived soils or that C_4 vegetation had successfully displaced C_3 in crevasse-splay environments by 4.8 Ma.

UBT-Psol 3 (2.42 Ma). The upper part of the Rohtas section is characterized by 15–20 m intervals of superimposed, yellow-brown floodplain paleosols, which alternate with 20–50-m-thick, multi-storied sand bodies (Fig. 5M). UBT-Psol 3 occurs near the middle of one of these stacked-soil sequences above a thin, laterally continuous, massive sandy silt that can be traced for over 400 m along strike. This soil is brown to yellow brown (10YR 4/3-3/3), leached of matrix carbonate, and includes cutans, mottles, fine root traces, uncommon Fe-Mn nodules, and dispersed $CaCO_3$ nodules that increase in size and abundance downward into the underlying sandy silt. Many of the paleosols in this sequence, including UBT-Psol 3, are capped by 10–20 cm of distinctive dark-brown to gray (10YR 4/1-4/2) silty clay, which we interpret as preserved A horizons.

Four samples from two sites along UBT-Psol 3 yielded $\delta^{13}C$ values of +2.9± 0.1‰, indicating C_4 vegetation grew on this soil at 2.4 Ma. Other paleosols within this sequence give similar results, and there is no indication of any remaining C_3 vegetation in a total of nine analyses of four different soils (Table 1; Fig. 10). Thus, sometime before 2.4 Ma, the floodplains in this part of the Siwalik foreland basin became dominated by C_4 grasses. Analogs to these C_4-dominated floodplain settings are extant in a few protected areas of lowland NW India and Nepal today (Mariotti and Peterschmitt, 1994; Quade et al., 1995).

Oxygen Isotopic Results and Discussion

The Oxygen Isotopic System in Soils

The oxygen isotopic composition ($\delta^{18}O$, PDB) of soil carbonate is determined mainly by the $\delta^{18}O$ value of soil water and temperature. However, the $\delta^{18}O$ value of soil carbonate in many modern soils does not show the predicted equilibrium offset from the $\delta^{18}O$ value of local, mean annual meteoric water at estimated mean annual soil temperatures (Quade et al., 1989b; Cerling and Quade, 1993). Additional considerations are the extent and mechanism by which water is removed from soils prior to the carbonate-forming event. Soils dewater by two non-fractionating processes affecting oxygen isotopes of soil water; that is, by filtration down and out of the soil profile and by plant transpiration and by one fractionating process in soil water: evaporation. Some modern soil carbonate can show substantial enrichments in $\delta^{18}O$ values, usually at shallow depths, which is probably the result of significant soil water evaporation accompanying soil carbonate formation (Quade et al., 1989b).

One interesting feature of modern soil carbonates in mixed C_3-C_4 ecosystems is the correlation between $\delta^{13}C$ and $\delta^{18}O$ values (Cerling, 1984; Quade et al., 1989b). A similar correlation seems to exist between $\delta^{13}C$ and $\delta^{18}O$ values in many long geologic sections spanning the late Neogene (Quade et al., 1995). To this we can add our Rohtas results, where a regression of $\delta^{13}C$ and $\delta^{18}O$ values from all paleosols yields an $r^2 = 0.51$. Is the correlation between $\delta^{13}C$ and $\delta^{18}O$ values in modern and ancient soils somehow related? The implication of the correlation in modern soils appears to be that soils underlying C_4 grassland may experience more heating and therefore evaporation than the average soil underlying a C_3 woodland or forest (Fig. 11). If correct, and no other factors contribute to $\delta^{18}O$ in soil H_2O, we would expect the $\delta^{18}O$ value of soil carbonate in samples from laterally continuous paleosols to cluster according to the type of vegetation that grew at the site, with low values under forest and higher average values under grasslands. We also would expect the $\delta^{18}O$ and $\delta^{13}C$ values to correlate along these lateral transects, as in modern mixed C_3-C_4 ecosystems soils.

Carbon and Oxygen Isotope Covariation

To examine the relationship between plant cover type and $\delta^{18}O_{carbonate}$ values, we regressed $\delta^{18}O_{carbonate}$ values against $\delta^{13}C_{carbonate}$ values in individual soils from the Rohtas section, to see if areas on the paleo-floodplain with greater grass abundance coincide with higher average $\delta^{18}O_{carbonate}$ values. Our lateral sampling of paleosols in the R15, R23, and R29 levels included areas once covered by forest and grassland, based on $\delta^{13}C$ results. We found only weak correlation ($r^2 = 0.01$–0.45) between $\delta^{18}O_{carbonate}$ and $\delta^{13}C_{carbonate}$ values in all soils except R15 Psol 6, where the $r^2 = 0.58$ for $\delta^{18}O_{carbonate}$ versus $\delta^{13}C_{carbonate}$ values, suggesting only a minor role of plants in modifying $\delta^{18}O_{sw}$ (sw—soil water) values (Data Repository item part 3; see footnote one). R15 Psol 6 is unique in that it is developed on floodplain deposits grading laterally into slightly coarser (sandy to clayey silt) channel fill, and the low $\delta^{18}O_{carbonate}$ and $\delta^{13}C_{carbonate}$ values occur on the channel fill portion of this paleosol. The association of the low isotopic values and a topographically lower channel-fill swale suggests that this was a more consistently moist and perhaps shaded part of the floodplain, with greater plant transpiration and less direct evaporation than contemporaneous soils that occurred laterally on the adjacent floodplain (Fig. 11).

Variations in $\delta^{18}O$ Values through Time

$\delta^{18}O$ (PDB) values show considerable (4–5‰) ranges in individual paleosols, but also a steady increase up-section (Figs. 7B and 10; Data Repository item parts 2 and 3 [see footnote 1]). This change is visible as a ~4‰ increase in the mean $\delta^{18}O$ (PDB) values of individual soils and similar increases in the minimum and maximum values. The mean $\delta^{18}O$ (PDB) values between paleosols at all stratigraphic intervals differ at the 95% confidence level (*t*-test) except between R15 and R23 (Data Repository item part 3).

Increases in the $\delta^{18}O$ (PDB) values of soil carbonate during the Neogene are evident in many sections globally, including other Siwalik sections (Fig. 7B), but the causes are unclear. We can eliminate the direct role of plants in modifying soil water $\delta^{18}O$ values in the Rohtas study, as discussed earlier. Other explanations include the impact of change in some aspect of climate (e.g., temperature, rainfall, or seasonality) on $\delta^{18}O_{sw}$ values over the past 8 m.y., perhaps related to the expansion of C_4 grass biomass.

Potential influences that we can definitely eliminate include local altitude and distance from the ocean, which have not changed appreciably during the Neogene (Tauxe and Opdyke, 1982).

The increase in $\delta^{18}O_{carbonate}$ values that we observe over the past 8 m.y. at Rohtas is embedded in larger and more dramatic increase in $\delta^{18}O_{carbonate}$ values in soils over the past 18 m.y. (Quade and Cerling, 1995). Dettman et al. (2001), studying fossil mollusks from the Siwaliks in Nepal, related the increases in $\delta^{18}O_{carbonate}$ values of ~4‰ during the Late Neogene to a gradual decrease in rainfall over the past 11 m.y., based on the well-known inverse relationship between rainfall amount and the $\delta^{18}O_{meteoric\ water}$ at low latitudes ("the amount effect"). Our results are consistent with this evidence, indicating an overall decrease in rainfall amount through the Rohtas sequence.

Implications for Floodplain Paleoecology

Relationship of Stable Isotopes and Floodplain Environments through Time

We examined the $\delta^{13}C$ values of the carbonate-bearing paleosols in the three distinct paleoenvironmental contexts: floodplain, crevasse-splay, and channel fill, to test for lithofacies association with different vegetation types and for changes in these associations through time (Figs. 4, 7, 10, and 12). Prior to 8.0 Ma and after 4.0 Ma, the low variability of $\delta^{13}C$ values from these different contexts indicates that vegetation on the aggrading alluvial plain was relatively homogeneous, with woodland or C_3 grassland vegetation prior to 8.0 Ma and C_4 grasslands dominant after 4.0 Ma (Fig. 7). However, during the Siwalik C_3-C_4 transition there was marked variability in the $\delta^{13}C$ value, indicating a mosaic of habitats with differences in the proportion of C_3 and C_4 vegetation. This variability is linked to the paleoenvironmental context of the paleosols (Fig. 12); after the beginning of the C_3-C_4 transition, red floodplain soils at the R15 and R29 levels supported the greatest proportion of C_4 grasslands while yellow-brown floodplain soils, crevasse-splays and channel fills supported trees and other woody plants as well as grass. This pattern occurs at several different stratigraphic levels, suggesting that depositional environment and substrate moisture played an important role in maintaining patches of C_3 and C_4 vegetation during ~4 m.y. of change from a C_3- to C_4-dominated fluvial ecosystem (Fig. 12). These habitat patches were at least hundreds of meters in diameter, judging by the lateral consistency of the $\delta^{13}C$ values, and could change through the lifetime of the soil (≤10 k.y.) based on evidence for vertical shifts in $\delta^{13}C$ values within individual soils.

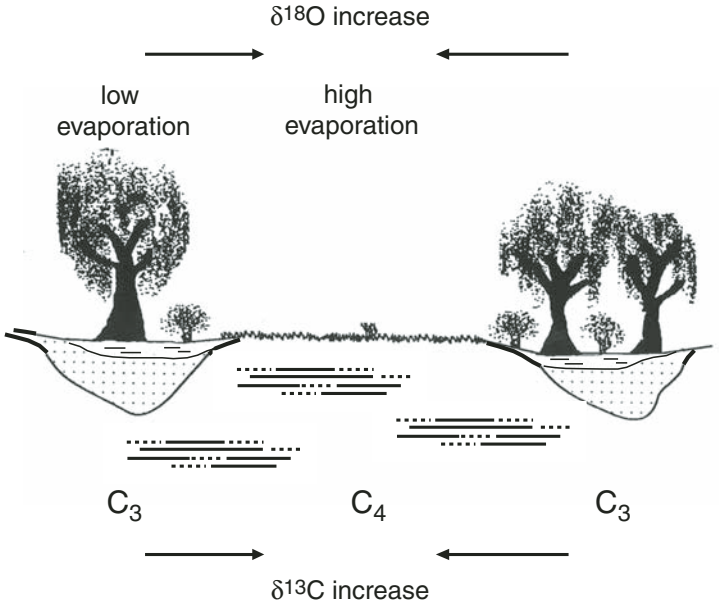

Figure 11. Schematic concept model for controls on oxygen and carbon isotopic variation across paleosols. Abandoned channel fills would likely retain more moisture during the dry season, in part because of the underlying water-charged sand bodies, which would encourage woody (C_3) vegetation with long vertical tap roots (Cole and Brown, 1976). This in turn would lower the evaporative stress in these settings relative to more open floodplain environments, resulting in lower $\delta^{18}O$ values.

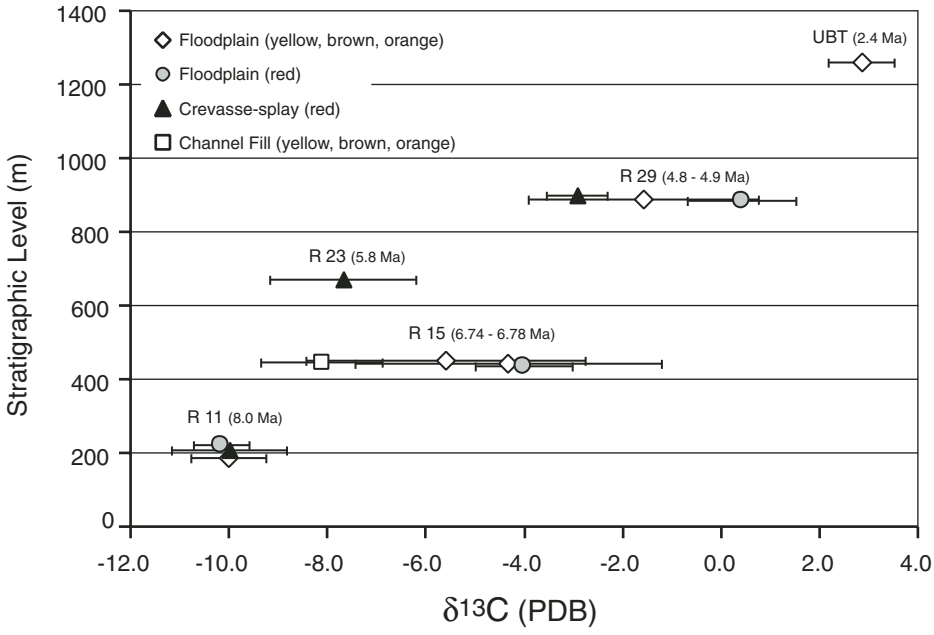

Figure 12. Summary of results for each sampled stratigraphic level at Rohtas, showing differences in the $\delta^{13}C$ (Peedee belemnite [PDB]) values for four types of paleosols in three different depositional contexts (floodplain, crevasse splay, channel fill). $\delta^{13}C$ values from paleosol carbonates in all three contexts indicate the dominance of C_3 vegetation before the beginning of the Siwalik C_3-C_4 transition (R11) (Data Repository item part 2, Table DR4 and part 3, Table DR8). During the transition, $\delta^{13}C$ values from channel fill and crevasse-splay soils remain more negative (more C_3 plants), whereas $\delta^{13}C$ values from red floodplain soils are more positive (more C_4 plants), evidence for local substrate control on the late Miocene vegetation mosaic.

The appearance of yellow-brown paleosols in the R15 level is the most distinctive stratigraphic marker in the Rohtas sequence, and the same color change has been noted in other Pakistan Siwalik sections (Quade and Cerling, 1995). Other pedogenic features (abundance of carbonate and Fe-Mn nodules, clay cutans, slickensides, and root and burrow traces) are remarkably stable through the Rohtas section, within paleosols from each of the environmental contexts (floodplain, crevasse-splay, channel fill), suggesting that the color change is superimposed on these environments and has little correlation with other paleosol characteristics. Although the yellow soil color makes its first appearance near the beginning of the shift from C_3- to C_4-dominated vegetation, this soil type has a range of $\delta^{13}C$ values during the Siwalik C_3-C_4 transition (Fig. 7; Table 1) and is not consistently associated with high $\delta^{13}C$ values (i.e., abundant C_4 plants). Intensely red paleosols with abundant carbonate are more predictably associated with higher $\delta^{13}C$ values from the R15 level upward than the yellow-brown soils, and the first red soil with a strong C_4 vegetation occurs ~3 m below the first of the yellow-brown soils. We did not find any consistent upward trend in the amount or position of pedogenic carbonate within the paleosols at Rohtas, in contrast to the observation by Johnson et al. (1981) of increased carbonate ("kankar"), indicating a shift to more seasonally arid conditions in the upper part of the Siwalik sequence.

Detailed analysis of Fe mineralization in the Siwalik paleosols is beyond the scope of this study. We suggest, however, that the yellow soils and carbonaceous A horizons could reflect a change in the balance of pedogenic iron oxides, from hematite in the red soils to goethite and other ferric oxyhydroxides that formed under periodically (e.g., seasonally) reducing conditions in the yellow soils (Schwertmann and Murad, 1983). These soils thus could reflect annual fluctuations in highly productive, seasonally water-saturated, edaphic grasslands that also were periodically dry enough for pedogenic carbonate precipitation. Later in the lifetime of the aggrading soil, a relatively lower water table and seasonally drier conditions would have allowed the growth of other types of vegetation, including bushes and trees. Today, these types of edaphic grasslands occur on the Indo-Gangetic Plain, forming dense ground cover and a well-developed A horizon (Deshpande et al, 1971a, 1971b; Lehmkuhl, 1994). Our isotopic results indicate that the yellow soils were common in topographically lower areas of the Miocene floodplains after 6.8 Ma, and also that drier grassland habitats were associated with the highly oxidized, carbonate-rich red soils. Moreover, during the C_3-C_4 transition, there is evidence for a temporal succession from edaphic grasslands to woodier vegetation *within* R15-Psol 6 and R29-Psol 2, which is consistent with gradual drying of soils in local topographic lows as these areas continued to aggrade. In more extreme cases of heat and water stress (e.g., lower water table during the dry season), C_4 grasses dominated the floodplain environments and trees were confined to deep, seasonally aerated soils formed on abandoned channel swales (e.g., the R15-Psol 6 channel fill).

The red crevasse-splay soils lag behind the other soil types in the transition from C_3 to C_4 vegetation (Fig. 12). It appears that until ca. 5 Ma this environment supported shrubs or other C_3 plants when most of the surrounding floodplain was inhabited by C_4 grasses. This may relate to the availability of more dry-season moisture in the underlying laminated silts and sands of the crevasse-splays than in the floodplain clayey silts, or possibly to rapid colonization of the unstable crevasse-splay surfaces by C_3 vegetation.

Distribution of C_3 versus C_4 Vegetation

It is clear that R11 Psol 1 represents pre-transition C_3 floodplain vegetation at 8.0 Ma, and UBT Psols 1–4 represent post-transition C_4 floodplain vegetation at 2.4 Ma (Fig. 10; Table 1). Returning to models in Figure 8, the isotopic evidence supports different distributions of C_3 versus C_4 vegetation at different times during the Siwalik C_3-C_4 transition (Fig. 7). The $\delta^{13}C$ distribution patterns in R15 Psol 6, R23 Psol 2, and R29 Psol 5 support Scenerio A; i.e., stable, 100-m-scale patches of C_3 or C_4 plants that did not migrate significantly during the time of soil formation. These patches coincided with channel-fill and crevasse-splay environments, indicating sustained local environmental control on woody versus grassy habitats. The isotopic results for the floodplain component of R15 Psol 6 and for R29 Psol 2 show vertical trends through time and support Scenerio B; i.e., patches of C_3 and C_4 plants that shifted on the landscape relative to the time of soil formation. These trends are analogous to shifts in forest-savanna ecotones that have been documented using $\delta^{13}C$ profiles in organic carbon from modern soils (Ambrose and Sikes, 1991; Mariotti and Peterschmitt, 1994; Desjardins et al., 1996). For the other paleosols that appear to have supported both C_3 and C_4 vegetation, based on the average and range of $\delta^{13}C$ results (R15 Psol 2, R29 Psol 2; see also Data Repository item part 2 [see footnote 1]), it is not possible to distinguish between scenarios A and B; i.e., patches of the different vegetation shifting spatially through the life of the soil (B) or an even, fine-scale mix of C_3 and C_4 biomass (C).

Long-Term Ecosystem Change

Standard deviations of sample populations at each level at Rohtas show that floodplain vegetation diversity (as measured by the $\delta^{13}C$ proxy) is lowest in the oldest (8.0 Ma) and youngest (2.4 Ma) parts of the record (Table 1; Data Repository item part 2), reflecting essentially pure C_3 (mainly forest) and pure C_4 (all grass) vegetation, respectively. In intervening levels, habitat diversity is markedly higher, at least at our sampled scale of hundreds of meters laterally. These results document habitat-scale resolution for ecological change that likely would have had important consequences for the indigenous vertebrate faunas, providing a mix of forest, woodland, and grassland habitats on a scale of hundreds to thousands of meters over an prolonged time interval of ~4.0 m.y.

The ~60%–70% expansion of C_4 grasses apparent between R11 (8.0 Ma) and R29 (4.7 Ma) suggests an average expansion rate of ~2% per 10^5 yr. This is a very modest rate when compared to, for example, changes in vegetation across glacial-interglacial transitions, when whole ecosystems turned over completely on timescales of 10^4 yr. We proposed earlier in this paper that the lateral variability of C_3 and C_4 vegetation on the Siwalik floodplains during the Siwalik C_3-C_4 transition was controlled by variations in the available substrate moisture (water table) in different environments, which were linked intrinsically to the aggrading fluvial system. However, it is also possible that such differences could be related to climate cycles on time scales of 10^4–10^5 yr, superimposed on longer-term climate change. In either scenario, the presence of both C_3 and C_4 vegetation on the alluvial plain resulted in a prolonged interval of variability in habitat structure, and during this interval the ecological effects of both fluvial processes and climate cycles could have been expressed in rapidly shifting grassland-forest ecotones.

The evolution of Siwalik plant and animal species has been independently documented over the past century and a half (see Barry et al., 2002; Badgley et al., 2005). A period of mammalian species extinction and origination occurred between 7.7 and 6.0 Ma, during the Siwalik C_3-C_4 transition, with drier- and grassland-adapted mammals replacing more closed- and moist-habitat faunas that included the anthropoid genus *Sivapithecus* (ancestral to the modern Orangutan). Farther east, in the Surai and Muksar sections of Nepal (Quade et al., 1995), and also in the Bengal Fan record (France-Lanord and Derry, 1994), the beginning of the C_3-C_4 isotope transition occurs somewhat later, closer to 7.0 Ma, and it is not recorded until 2.0–3.0 Ma in the northeastern part of the Tibetan Plateau (Wang and Deng, 2005). This indicates regional

differences in the onset of the shift toward C_4 vegetation, with eastern areas of the Himalayan front lagging well behind western ones. Our results indicate that fauna of the western portion of the Siwalik foreland basin experienced a slow and spatially complex ecological transformation from forested to grassland habitats over several million years during the C_3-C_4 transition interval, rather than an abrupt shift from 100% forest to 100% grassland over a shorter time period.

CONCLUSIONS

Earlier research documented a sharply defined C_3 to C_4 transition in Pakistan between 8.0 and 5.0 Ma (Quade and Cerling, 1995). Our higher-resolution study provides refined calibration of the Siwalik C_3-C_4 transition and reveals the internal complexity of a prolonged (≥3 m.y.) shift from forest-woodland– to grass-dominated alluvial ecosystems in the sub-Himalayan region of Pakistan (Quade and Cerling, 1995). It furthermore suggests that undetected subkilometer-scale variability could occur in other late Neogene $\delta^{13}C$ and $\delta^{18}O$ records based on single vertical sampling profiles through long stratigraphic sequences (e.g., Latorre et al., 1997; Fox and Koch, 2004; but see Levin et al., 2004).

In the Rohtas section of northern Pakistan, the complexity of pedogenic $\delta^{13}C$ and $\delta^{18}O$ within individual paleosols documents the scale and composition of shifting habitats on the Siwalik floodplains, including the relationship of different types of vegetation to underlying substrates. At a local scale, stable isotope values and internal features of the paleosols appear to have been controlled by substrate moisture and topography, and these attributes were unaffected by the large-scale shift from blue-gray to buff fluvial systems through the Rohtas sequence. Paleosol features such as clay cutans, mottling, and pedogenic carbonate and Fe-Mn nodule development do not show any consistent pattern of change through time. Variability in $\delta^{13}C$ through this sequence indicates that the local topographic and sedimentological conditions were important in mediating the effects of the changing climate (Latorre et al., 1997; Pagani et al., 1999) or the impact of global pCO_2 change (Cerling et al., 1997) on vegetation over ~3.2 m.y.—prior to the dominance of C_4 ecosystems in the late Miocene–early Pliocene. During and after the main Siwalik C_3-C_4 transition, previously documented between 8.0 and 5.0 Ma (Fig. 7) (Quade et al., 1989a; Quade and Cerling, 1995), C_3 plants continued to occur in favorable floodplain and crevasse-splay environments (R29 level) until at least 4.8 Ma (Table 1). Lateral variation in $\delta^{18}O$ values also suggests local differences in soil evaporation that were mediated to some extent by C_3 versus C_4 vegetation growing in different depositional settings (Figs. 10 and 11; Data Repository item part 3 [see footnote 1]), but the overall positive shift in $\delta^{18}O$ through the Rohtas sequence is interpreted as primarily a result of decreasing rainfall (the "amount effect").

This research demonstrates that stable isotopes can unlock previously inaccessible information about the structure of Neogene paleolandscapes. Documenting lateral variability in pedogenic $\delta^{13}C$ and $\delta^{18}O$ through other long stratigraphic sequences could help to calibrate potential errors in single-sample vertical isotope records, while simultaneously providing new information on habitat distributions across ancient landscapes and changes in the scale and proportions of these habitats through time.

ACKNOWLEDGMENTS

We sincerely thank our many colleagues for their support and encouragement of this research, both during the fieldwork and thereafter. We are especially grateful to the director generals of the Geological Survey of Pakistan (GSP), as well as S. Mahmood Raza, Khalid Sheikh, and numerous other colleagues from the GSP who supported this research and have made possible our collaborative research over many decades. John Kappelman thanks Jon Stence, Tim Ryan, Paige Hake Sheehan, and Wulf Gose for laboratory assistance. Jay Quade and Kay Behrensmeyer thank Naomi Levin for laboratory work, John Barry for input on the interpretation of the magnetostratigraphic correlations, Catherine Badgley for ideas regarding fluvial paleoecology, and Bill Keyser for engineering essential field equipment. Jan Price and Lynda Klasky and the staff of the Desert Research Laboratory provided support essential to the completion of this manuscript. We thank Neal Tabor, Jonathan Wynn, and associate editor Matt Kohn for their thoughtful reviews of the manuscript. The research reported in this paper was supported by the Smithsonian's Foreign Currency Program (SFCP 7087120000-6) and the National Science Foundation (BNS 84-17903).

REFERENCES CITED

Ambrose, S.H., and Sikes, N.E., 1991, Soil carbon isotope evidence for Holocene habitat change in the Kenya rift valley: Science, v. 253, no. 5026, p. 1402–1405, doi: 10.1126/science.253.5026.1402.

Badgley, C.E., Nelson, S., Barry, J., Behrensmeyer, A.K., and Cerling, T., 2005, Testing models of faunal turnover with Neogene mammals from Pakistan, *in* Lieberman, D. E., Smith, R. J., Kelley, J., eds., Interpreting the past: Essays on human, primate, and mammal evolution, in honor of David Pilbeam: Boston, Brill Academic Publishers, American School of Prehistoric Research Monograph Series, p. 29–44.

Barry, J.C., Morgan, M.E., Flynn, L.J., Pilbeam, D., Behrensmeyer, A.K., Raza, S.M., Khan, I.A., Badgley, C., Hicks, J., and Kelley, J., 2002, Faunal and environmental change in the late Miocene Siwaliks of northern Pakistan: Paleobiology, v. 28, Memoir, v. 3, Supplement, p. 1–71.

Behrensmeyer, A.K., and Tauxe, L., 1982, Isochronous fluvial systems in Miocene deposits of northern Pakistan: Sedimentology, v. 29, p. 331–352, doi: 10.1111/j.1365-3091.1982.tb01799.x.

Behrensmeyer, A.K., Willis, B.J., and Quade, J., 1995, Floodplains and paleosols in the Siwalik Neogene and Wyoming Paleogene: Implications for the taphonomy and paleoecology of faunas: Palaeoecology, Palaeogeography, Palaeoclimatology, v. 115, p. 37–60, doi: 10.1016/0031-0182(94)00106-I.

Bernor, R.L., Scott, R.S., Fortelius, M., Kappelman, J., and Sen, S., S., 2003. Systematics and Evolution of the Late Miocene Hipparions from Sinap, Turkey, *in* Fortelius, M., Kappelman, J., Bernor, R., and Sen, S., eds., Geology and paleontology of the Sinap Formation, Turkey: New York, Columbia University Press, p. 220–281.

Burbank, D.W., and Beck, R.A., 1991, Models of aggradation versus progradation in the Himalayan Foreland: Geologische Rundschau, v. 80, p. 623–638, doi: 10.1007/BF01803690.

Cande, S.C., and Kent, D.V., 1995, Revised calibration of the geomagnetic polarity timescale for the Late Cretaceous and Cenozoic: Journal of Geophysical Research, v. 100, p. 6093–6095, doi: 10.1029/94JB03098.

Cerling, T.E., 1984, The stable isotopic composition of modern soil carbonate and its relationship to climate: Earth and Planetary Science Letters, v. 71, p. 229–240, doi: 10.1016/0012-821X(84)90089-X.

Cerling, T.E., and Quade, J., 1993, Stable carbon and oxygen isotopes in soil carbonates, *in* Swart, P., McKenzie, J.C., and Lohman, K.C., eds., Continental indicators of climate: Proceedings of Chapman Conference, Jackson Hole, Wyoming: American Geophysical Union Monograph 78, p. 217–231.

Cerling, T.E., Harris, J.M., and Passey, B.H., 2003, Diets of East African Bovidae based on stable isotope analysis: Journal of Mammalogy, v. 84, no. 2, p. 456–470, doi: 10.1644/1545-1542(2003)084<0456:DOEABB>2.0.CO;2.

Cerling, T.E., Quade, J., Wang, Y., and Bowman, J.R., 1989, Carbon isotopes in soils and paleosols as ecologic and paleoecologic indicators: Nature, v. 341, p. 138–139, doi: 10.1038/341138a0.

Cerling, T.E., Harris, J.M., MacFadden, B.J., Leakey, M.G., Quade, J., Eisenmann, V., and Ehleringer, J.R., 1997, Global vegetation change through the Miocene/Pliocene boundary: Nature, v. 389, p. 153–158, doi: 10.1038/38229.

Codron, J., Codron, D., Lee-Thorp, J.A., Sponheimer, M., Bond, W.J., de Ruiter, D., and Grant, R., 2005, Taxonomic, anatomical, and spatio-temporal variations in the stable carbon and nitrogen isotopic compositions of plants from an African savanna: Journal of Archaeological Science, v. 32, p. 1757–1772, doi: 10.1016/j.jas.2005.06.006.

Cole, M.M., and Brown, R.C., 1976, The vegetation of the Ghanzi area of western Botswana: Journal of Biogeography, v. 3, no. 3, p. 169–196, doi: 10.2307/3038009.

Crowe, J., Gose, W., and Kappelman, J., 1993, A paleomagnetics analysis program for Windows and Macintosh: Geological Society of America Abstracts with Programs, v. 25, no. 6, p. A-209.

Davidson, G.R., 1995, The stable isotopic composition and measurement of carbon in soil CO_2: Geochimica et Cosmochimca Acta, v. 59, no. 12, p. 2485–2489, doi: 10.1016/0016-7037(95)00143-3.

Desjardins, T., Filho, A.C., Mariotti, A., Girardin, C., and Chauvel, A., 1996, Changes of the forest-savanna boundary in Brazilian Amazonia during the Holocene revealed by stable isotope ratios of soil organic carbon: Oecologia, v. 108, p. 749–756, doi: 10.1007/BF00329051.

Deshpande, S.B., Fehrenbacher, J.B., and Beavers, A.H., 1971a, Mollisols of Teria region of Uttar Pradesh, northern India 1. Morphology and mineralogy: Geoderma, v. 6, p. 179–193, doi: 10.1016/0016-7061(71)90005-X.

Deshpande, S.B., Fehrenbacher, J.B., and Ray, B.W., 1971b, Mollisols of Teria region of Uttar Pradesh, northern India 2: Genesis and Classification: Geoderma, v. 6, p. 195–201.

Dettman, D.L., Kohn, M.J., Quade, J., Ryerson, F.J., Ojha, T.P., and Hamidullah, S., 2001, Seasonal stable isotope evidence for a strong Asian monsoon throughout the past 10.7 Ma: Geology, v. 29, p. 31–34, doi: 10.1130/0091-7613(2001)029<0031:SSIEFA>2.0.CO;2.

Fisher, R.A., 1953, Dispersion on a sphere: Proceedings of the Royal Society of London, v. 217, p. 295–305.

Fox, D., and Koch, P.L., 2004, Carbon and oxygen isotopic variability in Neogene paleosol carbonates: Constraints on the evolution of C_4 grasslands: Palaeoecology, Palaeogeography, Palaeoclimatology, v. 207, p. 305–329, doi: 10.1016/S0031-0182(04)00045-8.

France-Lanord, C., and Derry, C.L., 1994, Evolution of the Himalaya since Miocene time: Isotopic and

sedimentological evidence from the Bengal Fan: Geochimica et Cosmochimica Acta, v. 58, p. 4809–4814, doi: 10.1016/0016-7037(94)90210-0.

Garcés, M., Cabrera, L., Agustí, J., and Parés, J.M., 1997, Old World first appearance datum of "*Hipparion*" horses: Late Miocene large-mammal dispersal and global events: Geology, v. 25, p. 19–22, doi: 10.1130/0091-7613(1997)025<0019:OWFADO>2.3.CO;2.

Gile, L.H., Peterson, F.F., and Grossman, R.B., 1966, Morphological and genetic sequences of carbonate accumulation in desert soils: Soil Science, v. 101, p. 347–360, doi: 10.1097/00010694-196605000-00001.

Hoorn, C., Ojha, T.P., and Quade, J., 2000, Palynologic evidence for paleovegetation changes in the Sub-Himalayan zone of Nepal during the late Neogene: Palaeoecology, Palaeogeography, Palaeoclimatology, v. 163, p. 133–161, doi: 10.1016/S0031-0182(00)00149-8.

Johnson, G.D., 1977, Paleopedology of *Ramapithecus*-bearing sediments, North India: Geologischen Rundschau, v. 66, no. 1, p. 192–216, doi: 10.1007/BF01989572.

Johnson, G.D., Johnson, N.M., Opdyke, N.D., and Tahirkheli, R.A.K., 1979, Magnetic reversal stratigraphy and sedimentary tectonic history of the Upper Siwalik Group eastern Salt Range and southwestern Kashmir, *in* Farah, A. and DeJong, K.A., eds., Geodynamics of Pakistan: Quetta, Pakistan, Geological Survey of Pakistan, p. 149–165.

Johnson, N.M., Opdyke, N.D., and Lindsay, E.H., 1975, Magnetic polarity stratigraphy of Plio-Pleistocene terrestrial deposits and vertebrate faunas, San Pedro valley, Arizona: Geological Society of America Bulletin, v. 86, p. 5–12, doi: 10.1130/0016-7606(1975)86<5:MPSOPT>2.0.CO;2.

Johnson, G.D., Rey, P.H., Ardrey, R.H., Visser, C.F., Opdyke, N.D., and Tahirkheli, R.A.K., 1981, Paleoenvironments of the Siwalik Group, Pakistan and India, *in* Rapp, Jr., G., and Vondra, C.F., eds., Hominid sites: Their geologic settings: Boulder, Colorado, Westview Press, AAAS Selected Symposium 63, p. 197–254.

Johnson, G.D., Zeitler, P., Naeser, C.W., Johnson, N.M., Summers, D.M., Frost, C.D., Opdyke, N.D., and Tahirkheli, R.A.K., 1982a, The occurrence and fission-track ages of late Neogene and Quaternary volcanic sediments, Siwalik Group, northern Pakistan: Palaeogeography, Palaeoclimatology, Palaeoecology, v. 37, p. 63–93, doi: 10.1016/0031-0182(82)90058-X.

Johnson, N.M., Opdyke, N.D., Johnson, G.D., Lindsay, E.H., and Tahirkheli, R.A.K., 1982b, Magnetic polarity stratigraphy and ages of Siwalik Group rocks of the Potwar Plateau, Pakistan: Palaeogeography, Palaeoclimatology, Palaeoecology, v. 37, p. 17–42, doi: 10.1016/0031-0182(82)90056-6.

Johnson, N.M., Stix, J., Tauxe, L., Cervany, P.F., and Tahirkheli, R.A.K., 1985, Paleomagnetic chronology, fluvial processes, and tectonic implications of the Siwalik deposits near Chinji Village, Pakistan: The Journal of Geology, v. 93, p. 27–40.

Kappelman, J., Kelley, J., Pilbeam, D., Sheikh, K.A., Ward, S., Anwar, M., Barry, J.C., Brown, B., Hake, P., Johnson, N.M., Raza, S.M., and Shah, S.M.I., 1991, The earliest occurrence of *Sivapithecus* from the middle Miocene Chinji Formation of Pakistan: Journal of Human Evolution, v. 21, p. 61–73, doi: 10.1016/0047-2484(91)90036-U.

Kappelman, J., Sen, S., Fortelius, M., Duncan, A., Alpagut, B., Crabaugh, J., Gentry, A., Lunkka, J.P., McDowell, F., Solounias, N., Viranta, S., and Werdelin, L., 1996, Chronology and biostratigraphy of the Miocene Sinap Formation of central Turkey, *in* Bernor, R., Fahlbusch, V., and Rietschel, S., eds., Evolution of Neogene continental biotopes in central Europe and the eastern Mediterranean: New York, Columbia University Press, p. 78–95.

Khan, I.A., Bridge, J.S., Kappelman, J., and Wilson, R., 1997, Evolution of Miocene fluvial environments, eastern Potwar plateau, northern Pakistan: Sedimentology, v. 44, p. 221–251, doi: 10.1111/j.1365-3091.1997.tb01522.x.

Khan, M.A., Ahmed, R., Raza, H.A., and Kemal, A., 1986, Geology of Petroleum in Kohat-Potwar Depression, Pakistan: AAPG Bulletin, v. 70, p. 396–414.

Kleinert, K., and Strecker, M.R., 2001, Climate change in response to orographic barrier uplift: paleosol and stable isotope evidence from the late Neogene Santa Maria basin, northwestern Argentina: Geological Society of America Bulletin, v. 113, no. 6, p. 728–742, doi: 10.1130/0016-7606(2001)113<0728:CCIRTO>2.0.CO;2.

Latorre, C., Quade, J., and McIntosh, W.C., 1997, The expansion of C_4 grasses and global change in the late Miocene: stable isotope evidence from the Americas: Earth and Planetary Science Letters, v. 146, p. 83–96, doi: 10.1016/S0012-821X(96)00231-2.

Leamy, M.L., and Rafter, T.A., 1972, Isotope ratios preserved in pedogenic carbonate and their application in palaeopedology: Wellington, New Zealand, Proceedings of the 8th International Conference on Radio Carbon Dating, p. D42–57.

Lehmkuhl, J.F., 1994, A classification of subtropical riverine grassland and forest in Chitwan National Park, Nepal: Plant Ecology, v. 111, p. 29–43.

Levin, N., Quade, J., Simpson, S., Semaw, S., and Rogers, M., 2004, Isotopic evidence for Plio-Pleistocene environmental change at Gona, Ethiopia: Earth and Planetary Science Letters, v. 219, p. 93–100, doi: 10.1016/S0012-821X(03)00707-6.

Machette, M.N., 1985, Calcic soils of the southwestern United States, *in* Weide, D.L., ed., Soils and Quaternary geology of the Southwestern United States: Geological Society of America Special Paper 203, p. 1–22.

Mariotti, A., and Peterschmitt, E., 1994, Forest savanna ecotone dynamics in India as revealed by carbon isotope ratios of soil organic matter: Oecologia, v. 97, p. 475–480, doi: 10.1007/BF00325885.

Morgan, M.E., Kingston, J.D., and Marino, B.D., 1994, Carbon isotopic evidence for the emergence of C_4 plants in the Neogene from Pakistan and Kenya: Nature, v. 367, p. 162–165, doi: 10.1038/367162a0.

Nelson, S.V., 2007, Isotopic reconstructions of habitat change surrounding the extinction of *Sivapithecus*, a Miocene hominoid, in the Siwalik Group of Pakistan: Palaeogeography, Palaeoclimatology, Palaeoecology, v. 243, no. 1–2, p. 204–222, doi: 10.1016/j.palaeo.2006.07.017.

Opdyke, N.D., Lindsay, E., Johnson, G.D., Johnson, N., Tahirkheli, R.A.K., and Mirza, M.A., 1979, Magnetic polarity stratigraphy and vertebrate paleontology of the Upper Siwalik subgroup of northern Pakistan: Palaeogeography, Palaeoclimatology, Palaeoecology, v. 27, p. 1–34, doi: 10.1016/0031-0182(79)90091-9.

Opdyke, N.D., Johnson, N.M., Johnson, G.D., Lindsay, E.H., and Tahirkheli, R.A.K., 1982, Paleomagnetism of the Siwalik Formations of northern Pakistan and rotation of the Salt Range Décollement: Palaeogeography, Palaeoclimatology, Palaeoecology, v. 37, p. 1–15, doi: 10.1016/0031-0182(82)90055-4.

Pagani, M., Freeman, K.H., and Arthur, M.A., 1999, Late Miocene atmospheric CO_2 concentrations and expansion of C_4 grasses: Nature, v. 285, p. 876–879.

Pilbeam, D., Morgan, M., Barry, J., and Flynn, L., 1996, European MN units and the Siwalik faunal sequence of Pakistan, *in* Bernor, R., Fahlbusch, V., and Rietschel, S., eds., Evolution of Neogene continental biotopes in central Europe and the eastern Mediterranean: New York, Columbia University Press, p. 96–105.

Quade, J., and Cerling, T.E., 1995, Expansion of C_4 grasses in the late Miocene of northern Pakistan: Evidence from stable isotopes in paleosols: Palaeogeography, Palaeoclimatology, Palaeoecology, v. 115, p. 91–116, doi: 10.1016/0031-0182(94)00108-K.

Quade, J., and Roe, L.J., 1999, The stable-isotope composition of early ground-water cements from sandstone in paleoecological reconstruction: Journal of Sedimentary Research, v. 69, p. 667–674.

Quade, J., Cerling, T.E., and Bowman, J.R., 1989a, Development of the Asian monsoon revealed by marked ecologic shift in the latest Miocene of northern Pakistan: Nature, v. 342, p. 163–166, doi: 10.1038/342163a0.

Quade, J., Cerling, T.E., and Bowman, J.R., 1989b, Systematic variations in the carbon and oxygen isotopic composition of pedogenic carbonate along elevation transects in the southern Great Basin, United States: Geological Society of America Bulletin, v. 101, p. 464–475, doi: 10.1130/0016-7606(1989)101<0464:SVITCA>2.3.CO;2.

Quade, J., Cater, J.M.L., Ojha, T.P., Adam, J., and Harrison, T.M., 1995, Dramatic carbon and oxygen isotopic shift in paleosols from Nepal and late Miocene environmental change across the northern Indian sub-continent: Geological Society of America Bulletin, v. 107, p. 1381–1397, doi: 10.1130/0016-7606(1995)107<1381:LMECIN>2.3.CO;2.

Raynolds, R.G.H., 1981, Did the ancestral Indus flow into the Ganges drainage?: University of Peshawar Geology Bulletin, v. 14, p. 141–150.

Retallack, G.J., 1991, Miocene paleosols and ape habitats of Pakistan and Kenya: New York, Oxford University Press, Oxford Monographs on Geology and Geophysics No. 19, 346 p.

Schwertmann, U., and Murad, E., 1983, Effect of pH on the formation of goethite and hematite from ferrihydrite: Clays and Clay Minerals, v. 31, no. 4, p. 277–284, doi: 10.1346/CCMN.1983.0310405.

Sen, S., 1989, *Hipparion* datum and its chronologic evidence in the Mediterranean area, *in* Lindsay, E.H., Fahlbusch, V., and Mein, P., eds, European Neogene mammal chronology: New York, Plenum Press, p. 495–505.

Sikes, N.E., 1994, Early hominid habitat preferences in East Africa: Paleosol carbon isotopic evidence: Journal of Human Evolution, v. 27, p. 25–45, doi: 10.1006/jhev.1994.1034.

Stern, L.A., Johnson, G.D., and Chamberlain, C.P., 1994, Carbon isotope signature of environmental change found in fossil ratite eggshells from a South Asian Neogene sequence: Geology, v. 22, p. 419–422, doi: 10.1130/0091-7613(1994)022<0419:CISOEC>2.3.CO;2.

Stubblefield, P.R., 1993, Age estimate of the late Miocene carbon isotope shift in the Potwar Plateau of Pakistan based on paleomagnetic reversal stratigraphy [M.A. thesis]: The University of Texas at Austin, 90 p.

Swart, P.K., Burns, S.J., and Leder, J.J., 1991, Fractionation of the stable isotopes of oxygen and carbon in carbon dioxide during reaction of calcite with phosphoric acid as a function of temperature and technique: Chemical Geology, v. 86, p. 89–96.

Tauxe, L., and Badgley, C., 1984, Transition stratigraphy and the problem of remanence lock-in times in the Siwalik red beds: Geophysical Research Letters, v. 11, p. 611–613.

Tauxe, L., and Opdyke, N.D., 1982, A time framework based on magnetostratigraphy for the Siwalik sediments of the Khaur area, northern Pakistan: Palaeogeography, Palaeoclimatology, Palaeoecology, v. 37, p. 43–61, doi: 10.1016/0031-0182(82)90057-8.

Tauxe, L., Kent, D.V., and Opdyke, N.D., 1980, Magnetic components contributing to the NRM of Middle Siwalik red beds: Earth and Planetary Science Letters, v. 47, p. 279–284, doi: 10.1016/0012-821X(80)90044-8.

Wang, Y., and Deng, T., 2005, A 25 m.y. isotopic record of paleodiet and environmental change from fossil mammals and paleosols from the NE Margin of the Tibetan Plateau: Earth and Planetary Science Letters, v. 236, p. 322–338, doi: 10.1016/j.epsl.2005.05.006.

Watson, G.S., 1956, A test for randomness: Monthly Notices, Royal Astronomical Society Geophysical Supplement 7, p. 160–161.

Willis, B.J., 1993a, Ancient river systems in the Himalayan foredeep, Chinji village area, northern Pakistan: Sedimentary Geology, v. 88, p. 1–76, doi: 10.1016/0037-0738(93)90151-T.

Willis, B.J., 1993b, Evolution of Miocene fluvial systems in the Himalayan foredeep through a two kilometer-thick succession in northern Pakistan: Sedimentary Geology, v. 88, p. 77–121, doi: 10.1016/0037-0738(93)90152-U.

Willis, B.J., and Behrensmeyer, A.K., 1994, Architecture of Miocene overbank deposits in northern Pakistan: Journal of Sedimentary Research, v. B64, no. 1, p. 60–67.

Willis, B.J., and Behrensmeyer, A.K., 1995, Fluvial systems in the Siwalik Miocene and Wyoming Eocene: Palaeoecology, Palaeogeography, Palaeoclimatology, v. 115, p. 13–36, doi: 10.1016/0031-0182(94)00105-H.

Wynn, J.G., 2004, Influence of Plio-Pleistocene aridification on human evolution: Evidence from paleosols of the Turkana Basin, Kenya: American Journal of Physical Anthropology, v. 123, p. 106–118, doi: 10.1002/ajpa.10317.

Zaleha, M.J., 1997, Intra- and extrabasinal controls on fluvial deposition in the Miocene Indo-Gangetic foreland, northern Pakistan: Sedimentology, v. 44, p. 369–390, doi: 10.1111/j.1365-3091.1997.tb01530.x.

Manuscript Received 27 June 2006
Revised Manuscript Received 9 January 2007
Manuscript Accepted 31 January 2007

Printed in the USA